

# 1. Dimensionality of Signals

HTE - 12.09.2012

Given a signal set of  $M$  signals (waveforms) of  $s_1(t) \cdots s_M(t)$ , we wish to find a set of  $N$  orthonormalized basis functions  $\psi_1(t) \cdots \psi_N(t)$ , so that we can write  $s_1(t) \cdots s_M(t)$  in terms of  $\psi_1(t) \cdots \psi_N(t)$ . Note that after this operation of orthogonalization, we can represent  $s_1(t) \cdots s_M(t)$  in an  $N$  dimensional space where each (orthogonal) axis corresponds to one of  $\psi_1(t) \cdots \psi_N(t)$ . We chose  $m$  and  $n$  indexes such that  $1 \leq m \leq M$ ,  $1 \leq n \leq N$  and it is reasonable to assume that  $N \leq M$ .

It is imperative to understand that  $s_1(t) \cdots s_M(t)$  constitute the symbols (i.e. the grouping of binary waveforms and their assignments to certain symbols) of a particular modulation scheme.

A formal method of finding  $\psi_1(t) \cdots \psi_N(t)$  given  $s_1(t) \cdots s_M(t)$  is to use Gram-Schmidt Orthogonalization Procedure. This is described below in steps

## Gram-Schmidt Orthogonalization Procedure

1. We begin with  $s_1(t)$  and set  $\psi_1(t)$  as follows

$$\psi_1(t) = \frac{s_1(t)}{\sqrt{\mathcal{E}_1}} \quad (1.1)$$

where  $\mathcal{E}_1$  is the energy in  $s_1(t)$  and found from

$$\mathcal{E}_1 = \int_{-\infty}^{\infty} s_1^2(t) dt \quad (1.2)$$

This way  $\psi_1(t)$  is simply  $s_1(t)$  with normalized energy, i.e. unity energy. Note that we demand orthonormalized basis functions  $\psi_1(t) \cdots \psi_N(t)$  to have unit energy to avoid scaling problems (similar to Frequency Transforms)

2. To find  $\psi_2(t)$  we proceed as follows. We take  $s_2(t)$  and find its projection onto  $\psi_1(t)$  (axis) from

$$c_{21} = \int_{-\infty}^{\infty} s_2(t) \psi_1(t) dt \quad (1.3)$$

Then we subtract  $c_{21}\psi_1(t)$  from  $s_2(t)$  to get

$$d_2(t) = s_2(t) - c_{21}\psi_1(t) \quad (1.4)$$

Now  $d_2(t)$  is orthogonal to  $\psi_1(t)$  and  $\psi_2(t)$  can be found by normalizing its energy, hence

$$\psi_2(t) = \frac{d_2(t)}{\sqrt{\varepsilon_2}}, \quad \varepsilon_2 = \int_{-\infty}^{\infty} d_2^2(t) dt \quad (1.5)$$

Note that unlike  $\varepsilon_1$ ,  $\varepsilon_2$  does not correspond to the energy in  $s_2(t)$ , but rather it refers to the energy in  $d_2(t)$ .

3. In general, the  $n$ th orthonormalized basis function is obtained from

$$\begin{aligned} \psi_n(t) &= \frac{d_n(t)}{\sqrt{\varepsilon_n}}, \quad d_n(t) = s_n(t) - \sum_{i=1}^{n-1} c_{ni} \psi_i(t), \\ \varepsilon_n &= \int_{-\infty}^{\infty} d_n^2(t) dt, \quad c_{ni} = \int_{-\infty}^{\infty} s_n(t) \psi_i(t) dt \quad i = 1 \cdots n-1 \end{aligned} \quad (1.6)$$

4. So, the process in 3. is continued until we reach  $n = M$ , i.e. when all  $M$  waveforms are exhausted.

**Example 1.1** : Four signals, waveforms, i.e.,  $M = 4$  named as  $s_1(t) \cdots s_4(t)$  are given in Fig. 1.1, we are asked to find a set of orthonormalized basis functions  $\psi_1(t) \cdots \psi_N(t)$ , where  $N \leq 4$ . Before we tackle the solution, it is important to remind that our signals are defined piecewise over the given time intervals. This means that mathematical calculations must be made taking into these intervals, otherwise we will get inaccurate results. To be precise, we give the expressions for  $s_1(t) \cdots s_4(t)$ , based on the plots in Fig. 1.1a and split into the time intervals they occupy.

$$\begin{aligned} s_1(t) &= \begin{cases} 1 & 0 \leq t \leq 2 \\ 0 & \text{otherwise} \end{cases} & s_2(t) &= \begin{cases} 1 & 0 \leq t \leq 1 \\ -1 & 1 < t \leq 2 \\ 0 & \text{otherwise} \end{cases} \\ s_3(t) &= \begin{cases} -1 & 0 \leq t \leq 1 \\ 1 & 1 < t \leq 3 \\ 0 & \text{otherwise} \end{cases} & s_4(t) &= \begin{cases} 1 & 0 \leq t \leq 3 \\ 0 & \text{otherwise} \end{cases} \end{aligned} \quad (1.7)$$

**Solution** : As described above, first we find  $\psi_1(t)$

$$\psi_1(t) = \frac{s_1(t)}{\sqrt{\varepsilon_1}}, \quad \text{where } \varepsilon_1 = \int_{-\infty}^{\infty} s_1^2(t) dt = 2, \quad \text{hence } \psi_1(t) = \frac{s_1(t)}{\sqrt{2}} \quad (1.8)$$

Now we proceed to find  $c_{21} = 0$  from

$$c_{21} = \int_{-\infty}^{\infty} s_2(t) \psi_1(t) dt = 0 \quad (1.9)$$

This is because the overlapping parts of  $s_2(t)$  and  $\psi_1(t)$  are orthogonal. Then  $d_2(t) = s_2(t)$  and

$$\psi_2(t) = \frac{d_2(t)}{\sqrt{\varepsilon_2}} = \frac{s_2(t)}{\sqrt{\varepsilon_2}} = \frac{s_2(t)}{\sqrt{2}} \quad , \quad \text{since} \quad \varepsilon_2 = \int_{-\infty}^{\infty} s_2^2(t) dt = 2 \quad (1.10)$$

To evaluate  $\psi_3(t)$ , we need to compute  $c_{31}$  and  $c_{32}$  using (1.6), this way

$$\begin{aligned} c_{31} &= \int_{-\infty}^{\infty} s_3(t) \psi_1(t) dt = \int_0^2 s_3(t) \psi_1(t) dt = \frac{-1}{\sqrt{2}} \int_0^1 dt + \frac{1}{\sqrt{2}} \int_1^2 dt = 0 \\ c_{32} &= \int_{-\infty}^{\infty} s_3(t) \psi_2(t) dt = -\sqrt{2} \end{aligned} \quad (1.11)$$

Then

$$d_3(t) = s_3(t) - c_{32}\psi_2(t) = s_3(t) + \sqrt{2}\psi_2(t) \quad (1.12)$$

As seen from (1.12),  $d_3(t)$  is a waveform extending from  $t=2$  to  $t=3$  with unit energy, thus  $\psi_3(t) = d_3(t)$ .

Finally (again using (1.6)), we find that  $c_{41} = \sqrt{2}$ ,  $c_{42} = 0$ ,  $c_{43} = 1$ , then

$$d_4(t) = s_4(t) - c_{43}\psi_3(t) - c_{42}\psi_2(t) - c_{41}\psi_1(t) = s_4(t) - \psi_3(t) - \sqrt{2}\psi_1(t) = 0 \quad (1.13)$$

As can be verified by plotting  $d_4(t)$ . (1.13) means that we have reached the end of the orthogonalization process and the waveforms  $s_1(t) \cdots s_4(t)$  can adequately be represented by orthonormalized basis functions of  $\psi_1(t) \cdots \psi_3(t)$ . So in this example  $M = 4$ ,  $N = 3$ . For general  $M$  and  $N$ , the waveforms  $s_1(t) \cdots s_4(t)$  can be plotted in an  $N$  dimensional signal space, where any of  $s_m(t)$  in  $s_1(t) \cdots s_M(t)$  can be written in terms of the orthonormalized basis functions of  $\psi_1(t) \cdots \psi_N(t)$  as follows

$$s_m(t) = \sum_{n=1}^N s_{mn} \psi_n(t) \quad , \quad m = 1 \cdots M \quad , \quad s_{mn} = \int_{-\infty}^{\infty} s_m(t) \psi_n(t) dt \quad (1.14)$$

(1.14) means  $s_m(t)$  can be constructed from the components  $s_{mn}$  along different  $\psi_n(t)$ . Or alternatively, we can say that  $s_{mn}$  coefficients are the projections of  $s_m(t)$  along the axis of  $\psi_n(t)$ . In this manner we define the vectorial representation of  $s_m(t)$  as

$$\mathbf{s}_m = [s_{m1}, s_{m2}, \cdots, s_{mN}] \quad , \quad \int_{-\infty}^{\infty} s_m(t) s_n(t) dt = \mathbf{s}_m \cdot \mathbf{s}_n \quad , \quad d_{mn} = |\mathbf{s}_m - \mathbf{s}_n| \quad (1.15)$$

The integral in the middle means that the product of two signal waveforms corresponds to the vectorial inner product. For instance if  $s_m(t)$  and  $s_n(t)$  are orthogonal, then the inner product will be zero.  $d_{mn}$  refers to the distance between the ends of vectors  $\mathbf{s}_m$  and  $\mathbf{s}_n$ , which will be important from probability of error performance.

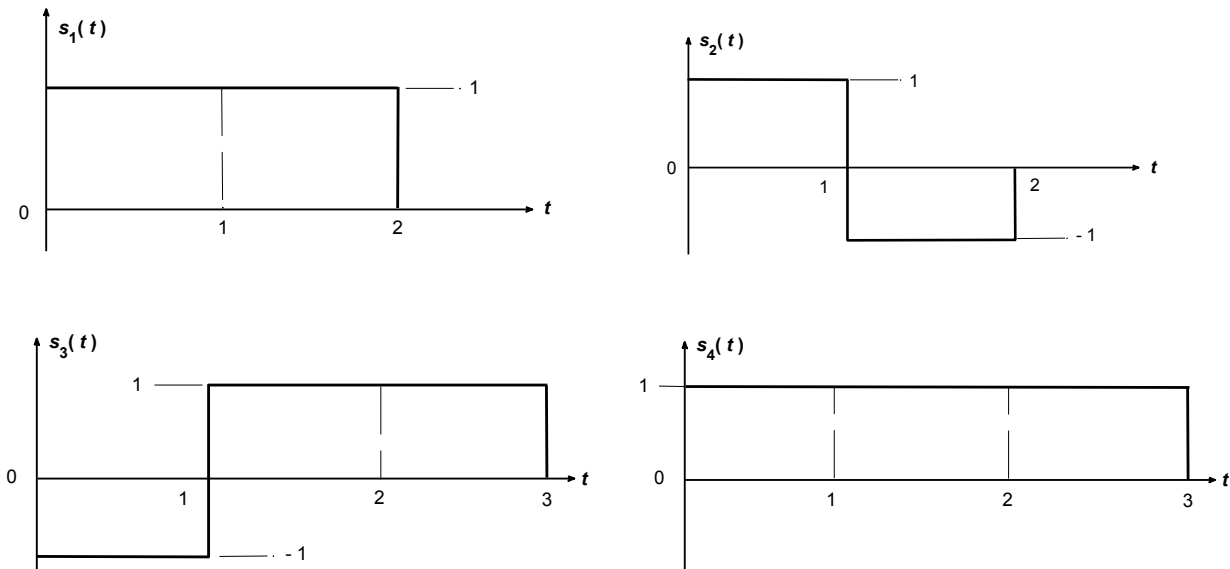
Since  $s_m(t)$  and  $\mathbf{s}_m$  refer to the same signal, the energy  $\varepsilon_m$  in  $s_m(t)$  can be obtained either from  $s_m(t)$  or from  $\mathbf{s}_m$ , thus

$$\varepsilon_m = \int_{-\infty}^{\infty} s_m^2(t) dt = \sum_{n=1}^N s_{mn}^2 = \|\mathbf{s}_m\|^2 \quad (1.16)$$

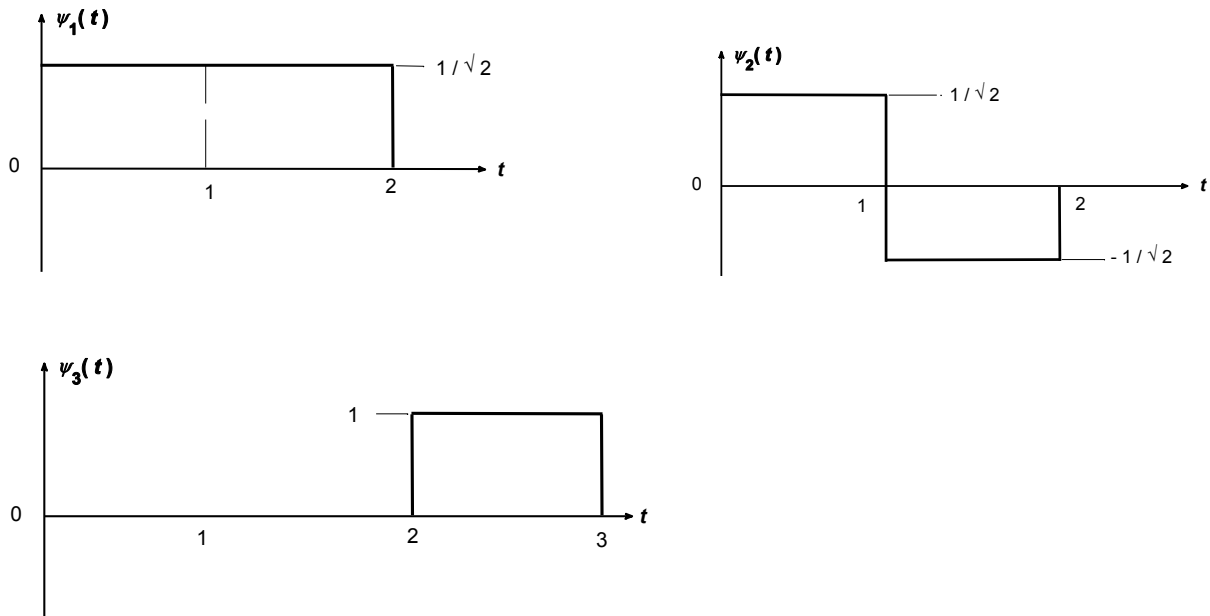
Note that it is important to comprehend these concepts, since they will be used in the detection process at receiver.

For the example above, signal vectors  $\mathbf{s}_1 \cdots \mathbf{s}_4$  are shown in Fig. 1.2 in the three dimensional space of  $\psi_1(t) \cdots \psi_3(t)$ . By using (1.14) and (1.15) it is possible to calculate  $\mathbf{s}_1 \cdots \mathbf{s}_4$  and their respective distances as

$$\begin{aligned} \mathbf{s}_1 &= \begin{bmatrix} \frac{s_{11}}{\sqrt{2}} & \frac{s_{12}}{0} & \frac{s_{13}}{0} \end{bmatrix}, \quad \mathbf{s}_2 = [0, \sqrt{2}, 0], \quad \mathbf{s}_3 = [0, -\sqrt{2}, 1], \quad \mathbf{s}_4 = [\sqrt{2}, 0, 1] \\ d_{12} &= |\mathbf{s}_1 - \mathbf{s}_2| = \left[ (\sqrt{2} - 0)^2 + (0 - \sqrt{2})^2 + (0 - 0)^2 \right]^{0.5} = 2, \quad d_{13} = |\mathbf{s}_1 - \mathbf{s}_3| = \sqrt{5} \\ d_{14} &= |\mathbf{s}_1 - \mathbf{s}_4| = 1, \quad d_{23} = |\mathbf{s}_2 - \mathbf{s}_3| = 3, \quad d_{24} = |\mathbf{s}_2 - \mathbf{s}_4| = \sqrt{5}, \quad d_{34} = |\mathbf{s}_3 - \mathbf{s}_4| = 2 \end{aligned} \quad (1.17)$$



a) Signal waveforms  $s_1(t) \cdots s_4(t)$



b) Orthonormal waveforms (basis function)  $\psi_1(t) \cdots \psi_3(t)$

Fig. 1.1 Signals waveforms and orthonormalized basis functions for Example 1.1

We do not always have to go to such lengths of finding orthonormalized basis functions by the use of **Gram-Schmidt Orthogonalization Procedure**. As an alternative, we can use intuition and eye inspection to arrive at a set of orthonormalized basis functions. Here the rule is that orthonormalized basis functions  $\psi_1(t) \cdots \psi_N(t)$  should satisfy three requirements

1.  $\psi_1(t) \cdots \psi_N(t)$  should be orthogonal amongst themselves, this means

$$\int_{-\infty}^{\infty} \psi_i(t) \psi_k(t) dt = 0 \quad \text{for } i \neq k, \quad i = 1 \cdots N, \quad k = 1 \cdots N \quad (1.18)$$

2.  $\psi_1(t) \cdots \psi_N(t)$  should have unit energy, this means

$$\int_{-\infty}^{\infty} \psi_n^2(t) dt = 1, \quad n = 1 \cdots N \quad (1.19)$$

3.  $\psi_1(t) \cdots \psi_N(t)$  should be able to represent (or span) all the signals in the set of  $s_1(t) \cdots s_M(t)$  in an  $N$  dimensional signal space, or alternatively we should be able to express all of the signal in the set of  $s_1(t) \cdots s_M(t)$  in terms of  $\psi_1(t) \cdots \psi_N(t)$ .

So bearing in mind these requirements and particularly paying attention to time slicing in wave forms of  $s_1(t) \cdots s_4(t)$ , we can deduce an alternative set of orthonormalized basis functions of  $\psi_1^a(t) \cdots \psi_3^a(t)$ , as shown in Fig. 1.3.

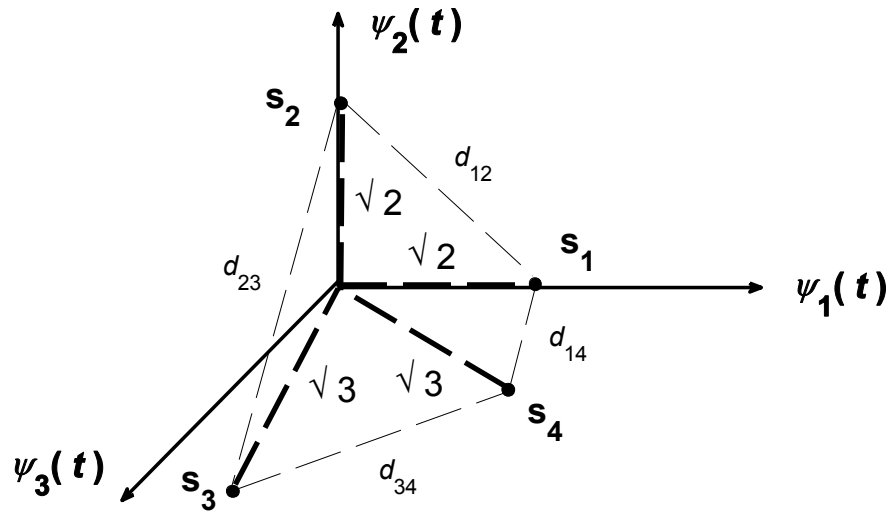


Fig. 1.2 Signal space diagram of signal waveforms  $s_1(t) \dots s_4(t)$  in Example 1.1.

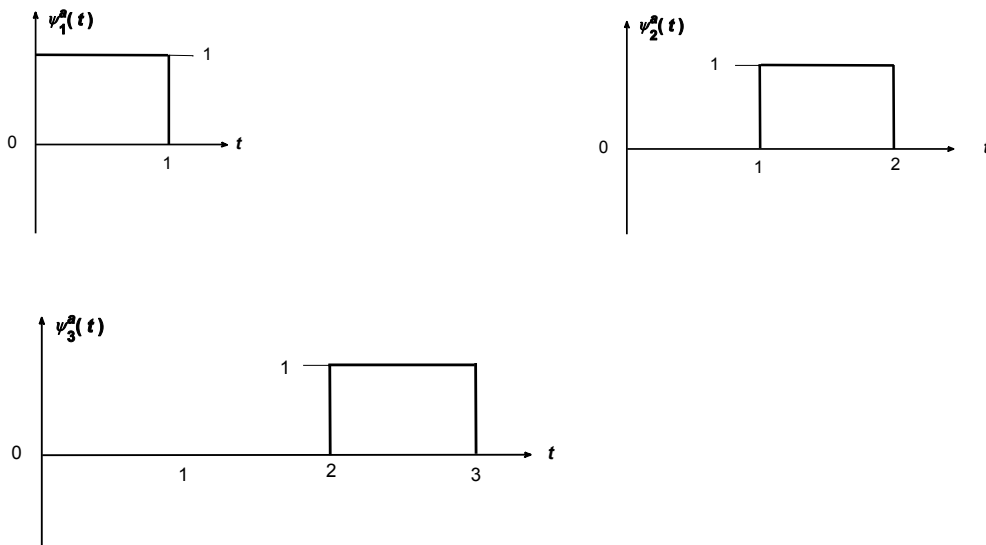


Fig. 1.3 Alternative set of orthonormalized basis functions of  $\psi_1^a(t) \dots \psi_3^a(t)$  for Example 1.1.

**Example 1.2 :** For the signal waveforms  $s_1(t) \dots s_4(t)$  given in Example 1.1, we can also find the orthonormalized basis functions  $\psi_1(t) \dots \psi_N(t)$  by using ECE376\_GSOthogonalWaveforms\_Exp4.m (available on course webpage, [ece376.cankaya.edu.tr](http://ece376.cankaya.edu.tr)). Below we illustrate how to represent  $s_1(t) \dots s_4(t)$  in that m file and how to interpret the results.

$$\begin{array}{c}
\text{Representation in Matlab} \\
0 \leq t \leq 1 \quad 1 \leq t \leq 2 \quad 2 \leq t \leq 3 \\
s_1(t) \cdots s_4(t) \rightarrow \text{stmat} = \begin{bmatrix} 1 & 1 & 0 \\ 1 & -1 & 0 \\ -1 & 1 & 1 \\ 1 & 1 & 1 \end{bmatrix} \begin{array}{l} \leftarrow s_1(t) \\ \leftarrow s_2(t) \\ \leftarrow s_3(t) \\ \leftarrow s_4(t) \end{array}
\end{array} \quad (1.20)$$

The stmat containing the time sliced form of  $s_1(t) \cdots s_4(t)$  is written on line 4 of ECE376\_GSOrthogonalWaveforms\_Exp1.m. In this manner (1.20) corresponds exactly to the signal waveform set given in Fig. 1.1a. After running ECE376\_GSOrthogonalWaveforms\_Exp4.m, we get the following output

$$\begin{array}{c}
\text{Representation in Matlab} \\
0 \leq t \leq 1 \quad 1 \leq t \leq 2 \quad 2 \leq t \leq 3 \\
\psi_1(t) \cdots \psi_N(t) \rightarrow \text{Fimat} = \begin{bmatrix} 0.7071 & 0.7071 & 0 \\ 0.7071 & -0.7071 & 0 \\ 0 & 0 & 1 \\ 0 & 0 & 0 \end{bmatrix} \begin{array}{l} \leftarrow \psi_1(t) \\ \leftarrow \psi_2(t) \\ \leftarrow \psi_3(t) \\ \leftarrow \psi_4(t) \end{array}
\end{array} \quad (1.21)$$

(1.21) is more or less self explanatory. The additional interpretations are Matlab finds exactly the result worked out by using Gram-Schmidt Orthogonalization Procedure, that is the orthonormalized waveforms of Fig. 1.1b. This is not surprising since ECE376\_GSOrthogonalWaveforms\_Exp4.m Matlab file follows (implements) the steps of Gram-Schmidt Orthogonalization Procedure given above. We can also use ECE376\_GSOrthogonalWaveforms\_Exp4.m to verify that orthonormalized waveforms have unit energy, they are orthogonal to each other and the vectorial representation, i.e.  $s_{mm}$  coefficients of the signal vectors as computed at the bottom of this Matlab file and written onto the workspace.

**Exercise 1.1 :** Find the representation of the signal set  $s_1(t) \cdots s_4(t)$  in terms of  $\psi_1^a(t) \cdots \psi_3^a(t)$ . Compare your new signal space diagram, signal vectors and the distances between their ends to those results of  $\psi_1(t) \cdots \psi_3(t)$ . Make your comments by plotting and writing for the relevant mathematical expressions. Do this by hand or by running the Matlab file ECE376\_GSOrthogonalWaveforms\_Exp4.m.

**Exercise 1.2 :** By using the Matlab file ECE376\_GSOrthogonalWaveforms\_Exp4.m (available on course webpage), find orthonormalized basis functions  $\psi_1(t) \cdots \psi_N(t)$  for the signal waveforms given in the Fig 1.4. Verify your results by hand derivation using Gram-Schmidt Orthogonalization Procedure or by eye inspection. Note that number of dimensions  $N$  cannot be greater than time slicing along  $t$  axis. Write your  $s_1(t) \cdots s_M(t)$  in terms of  $\psi_1(t) \cdots \psi_N(t)$ , draw the signal space diagram for this case.

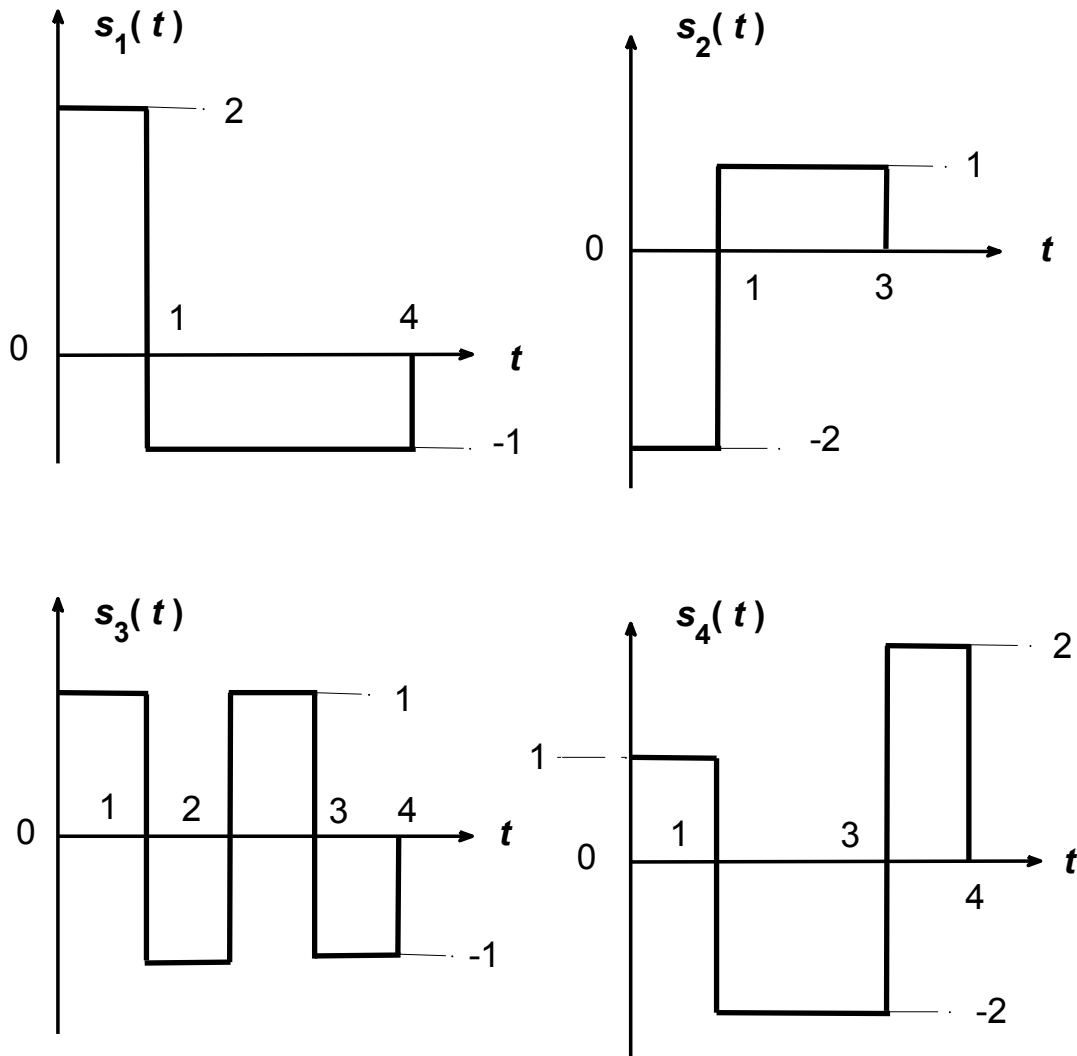


Fig. 1.4 Signal waveforms  $s_1(t) \cdots s_4(t)$  for Exercise 1.2.

Before we start to investigate different modulation types, it is instructive to show the simplified block diagram of the modulator we are referring to. This model is shown below in Fig. 1.5 including the prior part of analogue to digital conversion. According to this figure, modulation means taking unmodulated input of binary waveforms in groups of  $k = \log_2 M$  and converting (mostly called mapping) them into modulated output of  $M$  ary signals  $s_1(t) \cdots s_M(t)$ . The way that this modulator functions will correspond to different types of modulations examined next. Note that apart from the case of  $M = 2$ , it is always the case that (symbol duration)  $T > T_b$  (binary waveform duration). For this reason, strictly speaking, the energy of a symbol will increase as  $M$  is raised.

The relevant output waveforms from the blocks of Fig. 1.5 can be found in Fig. 1.6, for the sample cases of ASK and PSK at  $M = 4$ . Note that multilevel signal representation is modulation free, or modulationless. Hence a digital modulation block is assumed to be driven by a multilevel signal.



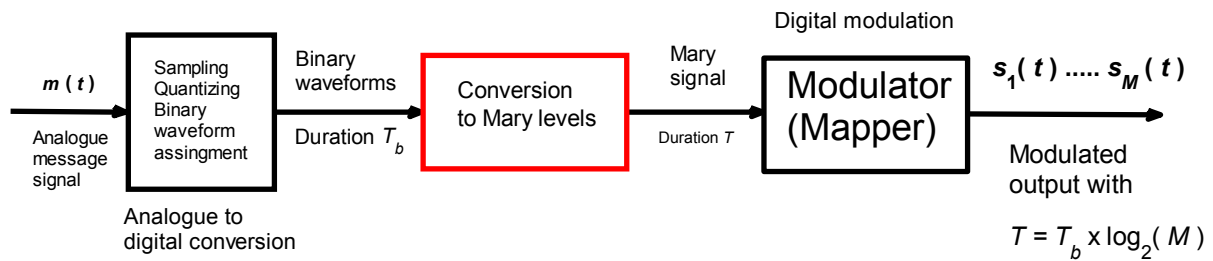


Fig. 1.5 Simplified block diagram of digital modulator including the prior part of analogue to digital conversion.

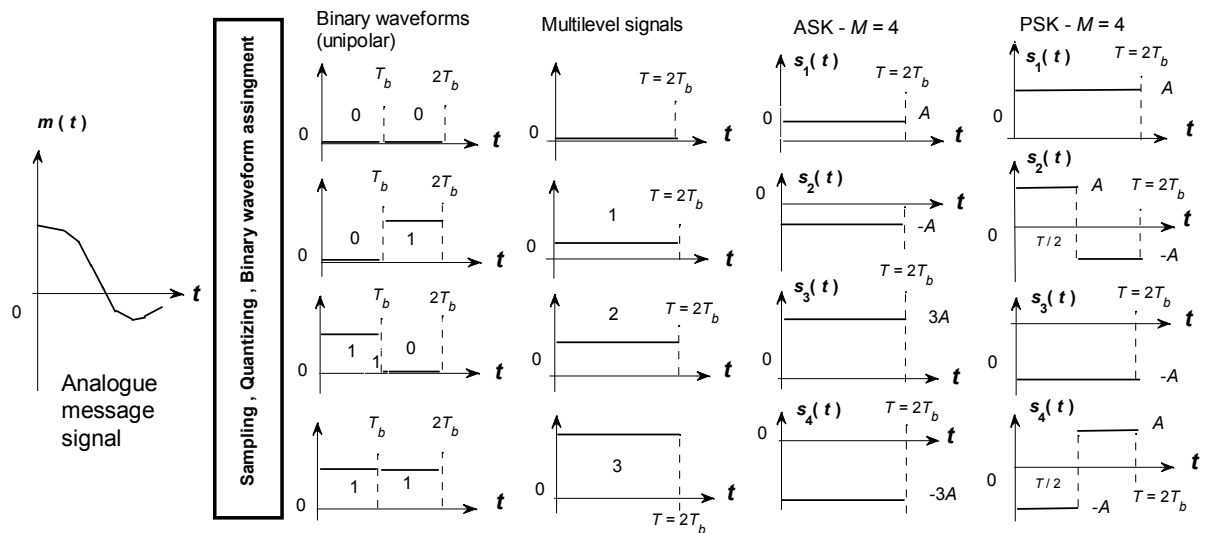


Fig. 1.6 Waveform representation of the outputs of the block in Fig. 1.5.

From Fig. 1.6, it is apparent, compared with ASK, PSK will demand more bandwidth, since it slices the symbol duration into two halves.

Below we take ASK, PSK and QAM in baseband form, since a sinusoidal carrier merely shifts the frequency spectrum of our modulated signal and has no effect on the probability of error analysis.

## 2. Amplitude Shift Keying (ASK) or Pulse Amplitude Modulation (PAM)

Now we examine different modulation types with the perspective of dimensionality of signal. The first and the simplest one is ASK (or PAM). In this modulation type,  $N = 1$ , so we say that ASK is one

dimensional, thus we need a single orthonormalized function  $\psi(t)$  which is usually drawn as a horizontal line, where the signal vectors are placed according to their respective energies. In this sense ASK signals will be differentiated by energy differences (essentially amplitude differences) and their respective orientation to the left (negative pulse) and to the right (positive pulse).

By taking a symbol duration of  $T$ , an ASK example of  $M = 4$  is given in Fig. 2.1

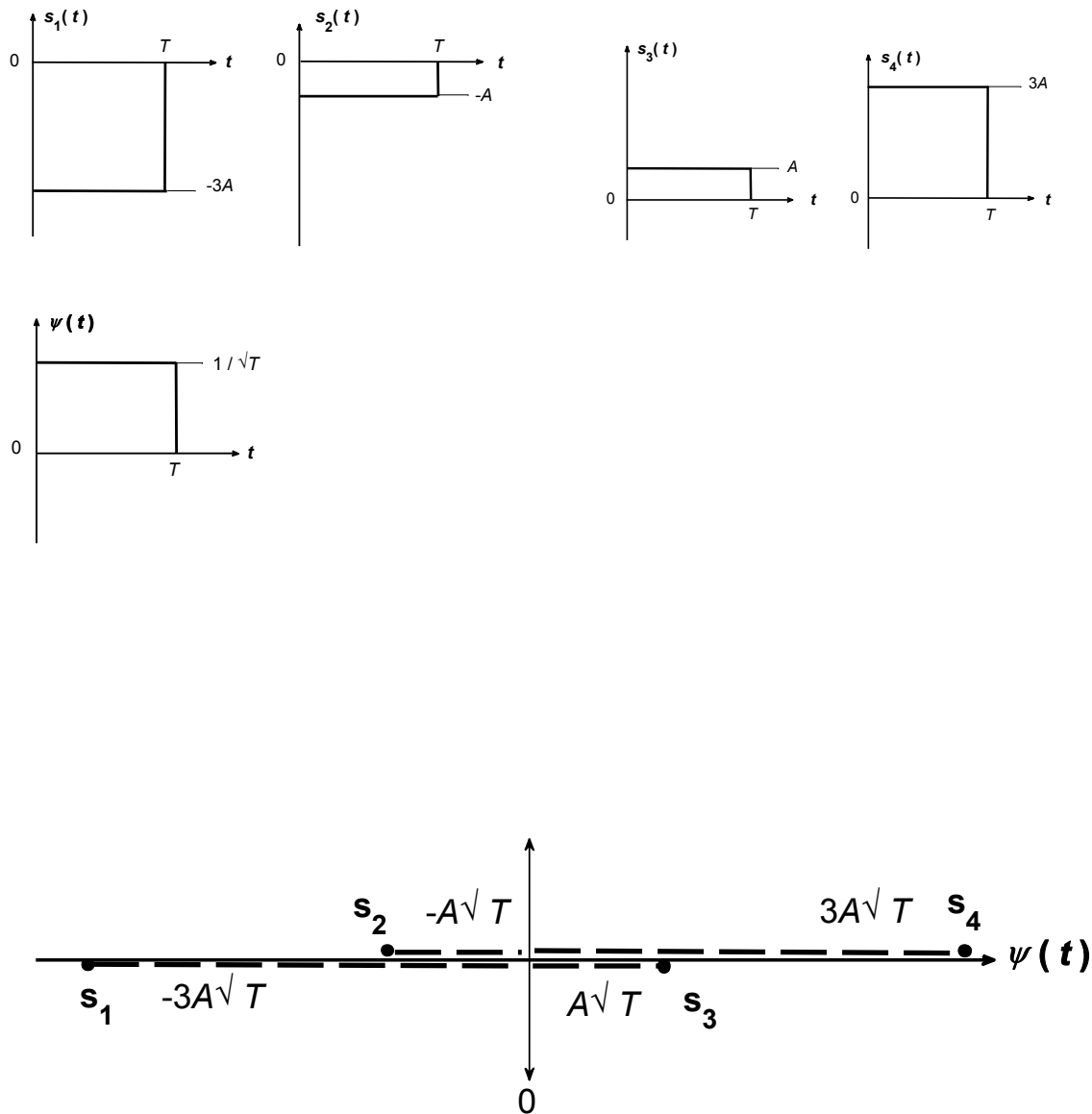


Fig. 2.1 An example of ASK signals, orthonormalized basis function and signal space diagram, for  $M = 4$ .

By looking at Fig. 2.1 and benefitting from the formulations given in section 1., it is possible to write the following expressions for signal waveforms  $s_1(t) \dots s_4(t)$ , signal vectors  $s_1 \dots s_4$  and their respective energies. This way  $s_1(t)$  and  $s_4(t)$  will have greater energies than  $s_2(t)$  and  $s_3(t)$

$$\begin{aligned}
s_1(t) &= -3A, \quad s_2(t) = -A, \quad s_3(t) = A, \quad s_4(t) = 3A, \quad \psi(t) = 1/\sqrt{T} \quad 0 \leq t \leq T \\
s_1(t) &= -3A\sqrt{T}\psi(t), \quad s_2(t) = -A\sqrt{T}\psi(t), \quad s_3(t) = A\sqrt{T}\psi(t), \quad s_4(t) = 3A\sqrt{T}\psi(t) \\
\mathbf{s}_1 &= [-3A\sqrt{T}], \quad \mathbf{s}_2 = [-A\sqrt{T}], \quad \mathbf{s}_3 = [A\sqrt{T}], \quad \mathbf{s}_4 = [3A\sqrt{T}] \\
\varepsilon_1 &= \|\mathbf{s}_1\|^2 = 9A^2T, \quad \varepsilon_2 = \|\mathbf{s}_2\|^2 = A^2T, \quad \varepsilon_3 = \|\mathbf{s}_3\|^2 = A^2T, \quad \varepsilon_4 = \|\mathbf{s}_4\|^2 = 9A^2T
\end{aligned} \tag{2.1}$$

Mostly to conserve bandwidth and to avoid intersymbol interference that will occur during transmission, we will not use rectangular waveforms, but instead use a shaping waveform called  $g_T(t)$ . We may set  $\psi(t)$  to be  $g_T(t)$ . The examples of rectangular and a sinusoidal shaped  $g_T(t)$  are mathematically given below

$$\begin{aligned}
\text{Rectangular shaping waveform } g_{TR}(t) &= \begin{cases} 1/\sqrt{T} & 0 \leq t \leq T \\ 0 & \text{otherwise} \end{cases} \\
\text{Sinusoidal shaping waveform } g_{TS}(t) &= \begin{cases} 2\sqrt{\frac{2}{3T}} \sin^2(\pi t/T) & 0 \leq t \leq T \\ 0 & \text{otherwise} \end{cases}
\end{aligned} \tag{2.2}$$

In Figs. 2.2 and 2.3, we show the respective time and frequency plots of the rectangular and sinusoidal shaping waveforms of (2.2).

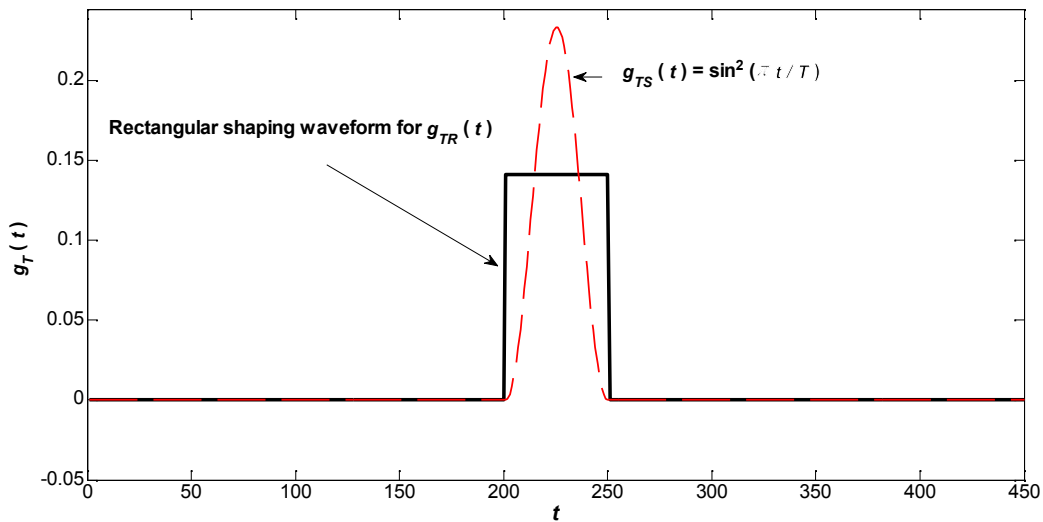


Fig. 2.2 Time plots of rectangular and sinusoidal shaping waveforms.

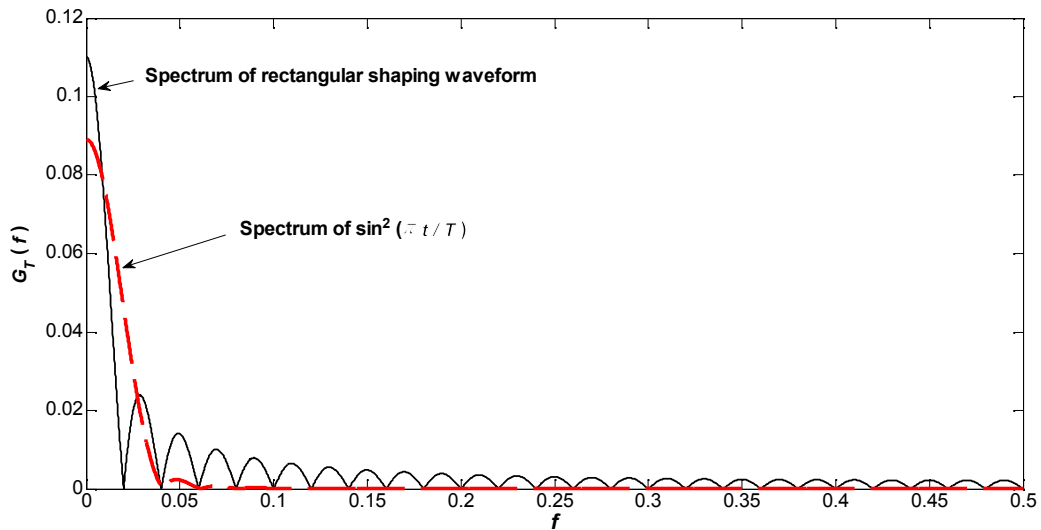
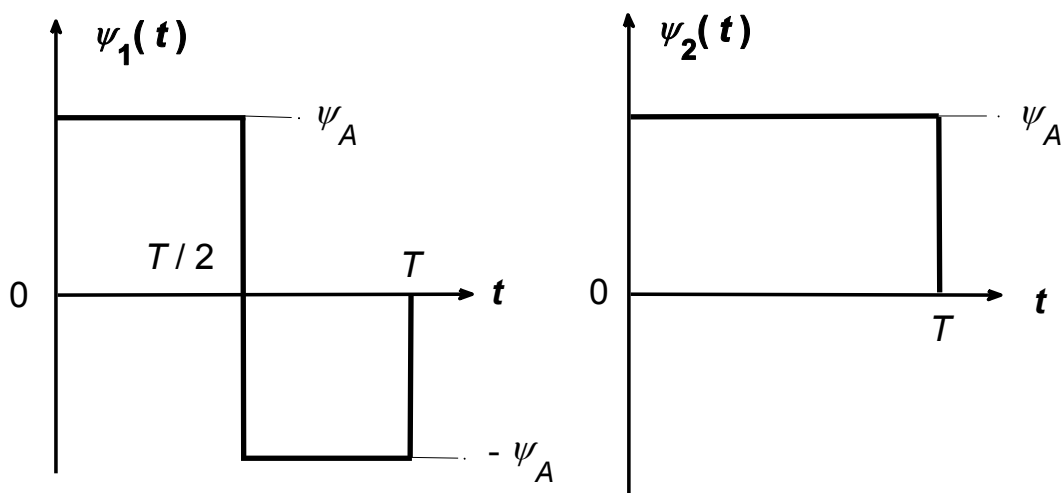


Fig. 2.3 Frequency spectrum plots of rectangular and sinusoidal shaping waveforms.

### 3. Phase Shift Keying (PSK) and Quadrature Amplitude Modulation (QAM) – Two Dimensional Signals

To establish two dimensions, it is natural to use two (orthogonal) axes which will be  $\psi_1(t)$  and  $\psi_2(t)$ . By taking a symbol duration of  $T$ , it is possible to generate two types of orthogonal set of  $\psi_1(t)$  and  $\psi_2(t)$  as illustrated in Fig. 3.1.



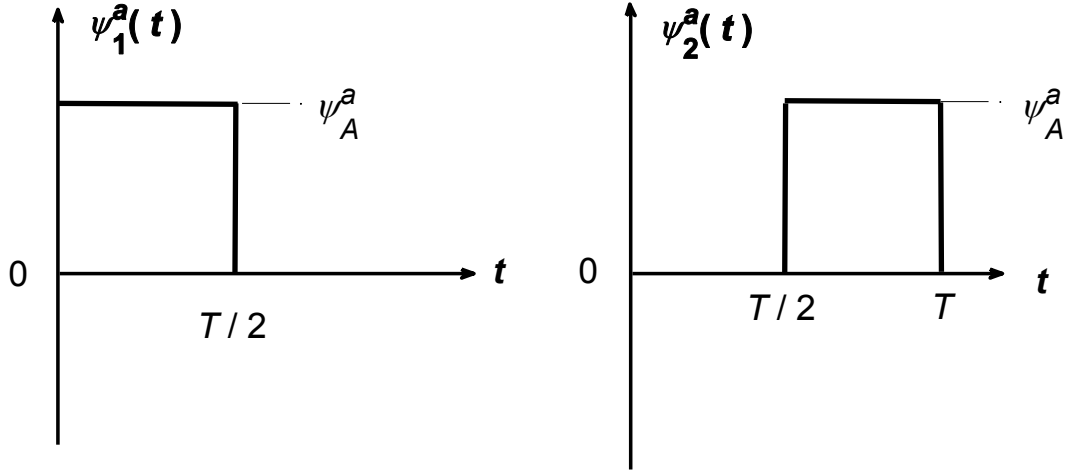


Fig. 3.1 Two sets orthogonal functions  $\psi_1(t)$  and  $\psi_2(t)$ ,  $\psi_1^a(t)$  and  $\psi_2^a(t)$ .

We can write the mathematical expressions of  $\psi_1(t)$  and  $\psi_2(t)$ ,  $\psi_1^a(t)$  and  $\psi_2^a(t)$  as

$$\begin{aligned}
 \psi_1(t) &= \psi_A \text{ for } 0 \leq t \leq T/2, \quad \psi_1(t) = -\psi_A \text{ for } T/2 \leq t \leq T, \quad \psi_1(t) = 0 \text{ for } t < 0 \text{ or } t > T \\
 \psi_2(t) &= \psi_A \text{ for } 0 \leq t \leq T, \quad \psi_2(t) = 0 \text{ for } t < 0 \text{ or } t > T \\
 \psi_1^a(t) &= \psi_A^a \text{ for } 0 \leq t \leq T/2, \quad \psi_1^a(t) = 0 \text{ for } t < 0 \text{ or } t > T/2 \\
 \psi_2^a(t) &= \psi_A^a \text{ for } T/2 \leq t \leq T, \quad \psi_2^a(t) = 0 \text{ for } t < T/2 \text{ or } t > T
 \end{aligned} \tag{3.1}$$

It is quite easy to see that

$$\int_{-\infty}^{\infty} \psi_1(t) \psi_2(t) dt = 0, \quad \int_{-\infty}^{\infty} \psi_1^a(t) \psi_2^a(t) dt = 0 \tag{3.2}$$

So both  $\psi_1(t)$  and  $\psi_2(t)$  and  $\psi_1^a(t)$  and  $\psi_2^a(t)$  are orthogonal among themselves. Note that  $\psi_1^a(t)$  and  $\psi_2^a(t)$  achieves orthogonalization by nonoverlapping along time axis, while  $\psi_1(t)$  and  $\psi_2(t)$  are overlapping. To establish that  $\psi_1(t)$  and  $\psi_2(t)$  and  $\psi_1^a(t)$  and  $\psi_2^a(t)$  are orthonormalized as well, we demand that energies are unity such that

$$\int_{-\infty}^{\infty} \psi_1^2(t) dt = 1, \quad \int_{-\infty}^{\infty} \psi_2^2(t) dt = 1, \quad \int_{-\infty}^{\infty} [\psi_1^a(t)]^2 dt = 1, \quad \int_{-\infty}^{\infty} [\psi_2^a(t)]^2 dt = 1 \tag{3.3}$$

From the evaluations in (3.2), we get  $\psi_A = \frac{1}{\sqrt{T}}$  and  $\psi_A^a = \sqrt{\frac{2}{T}}$ . So now  $\psi_1(t)$  and  $\psi_2(t)$  and  $\psi_1^a(t)$  and  $\psi_2^a(t)$  are both orthogonal and orthonormalized.

Now we choose two time signal waveforms  $s_1(t)$  and  $s_2(t)$ , similar to  $\psi_1(t)$  and  $\psi_2(t)$  as displayed in Fig. 3.2.

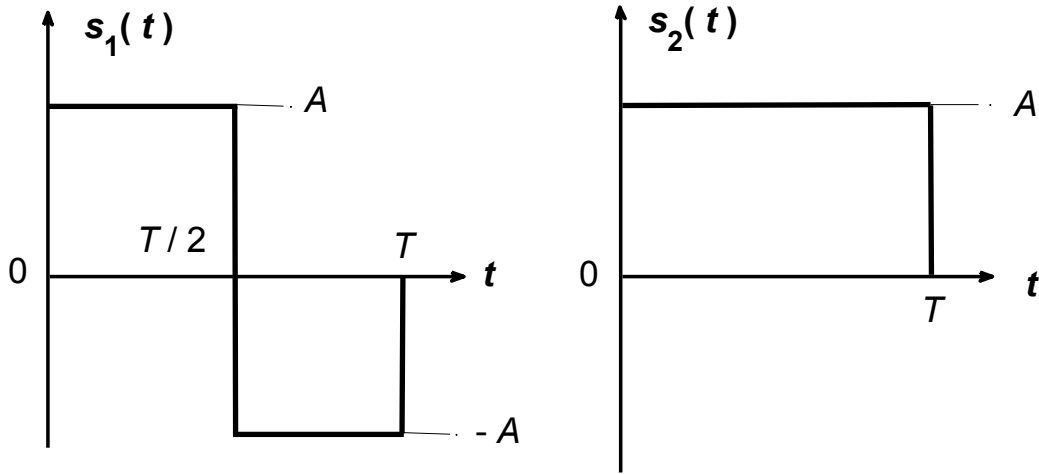


Fig. 3.2 Two time signal waveforms  $s_1(t)$  and  $s_2(t)$ .

If  $\psi_1^a(t)$  and  $\psi_2^a(t)$  are selected to represent  $s_1(t)$  and  $s_2(t)$ , then it is possible to write  $s_1(t)$  and  $s_2(t)$  in terms of the orthonormalized basis functions  $\psi_1^a(t)$  and  $\psi_2^a(t)$  as

$$s_1(t) = A \text{ for } 0 \leq t \leq T/2, s_1(t) = -A \text{ for } T/2 \leq t \leq T, s_1(t) = 0 \text{ for } t < 0 \text{ or } t > T$$

$$s_2(t) = A \text{ for } 0 \leq t \leq T, s_2(t) = 0 \text{ for } t < 0 \text{ or } t > T$$

$$s_1(t) = A\sqrt{\frac{T}{2}}\psi_1^a(t) - A\sqrt{\frac{T}{2}}\psi_2^a(t) \text{ for } 0 \leq t \leq T, s_1(t) = 0 \text{ for } t < 0 \text{ or } t > T$$

$$s_2(t) = A\sqrt{\frac{T}{2}}\psi_1^a(t) + A\sqrt{\frac{T}{2}}\psi_2^a(t) \text{ for } 0 \leq t \leq T, s_2(t) = 0 \text{ for } t < 0 \text{ or } t > T$$

$$\mathbf{s}_1 = [s_{11}, s_{12}] = \left[ A\sqrt{\frac{T}{2}}, -A\sqrt{\frac{T}{2}} \right], \mathbf{s}_2 = [s_{21}, s_{22}] = \left[ A\sqrt{\frac{T}{2}}, A\sqrt{\frac{T}{2}} \right] \quad (3.4)$$

Note that on the first two lines of (3.4), we have intentionally written for  $s_1(t)$  and  $s_2(t)$  as they are seen from  $s_1(t)$  and  $s_2(t)$  (without  $\psi_1^a(t)$  and  $\psi_2^a(t)$ ). On the third and fourth lines of (3.4), where there are the expressions of  $s_1(t)$  and  $s_2(t)$  in terms of  $\psi_1^a(t)$  and  $\psi_2^a(t)$ , we do not actually need the time range specifications given at the end of lines, since these time ranges are readily built into  $\psi_1^a(t)$  and  $\psi_2^a(t)$ . On the last line of (3.4) we have the vectorial representation of  $s_1(t)$  and  $s_2(t)$ , i.e.  $\mathbf{s}_1 = [s_{11}, s_{12}]$  and  $\mathbf{s}_2 = [s_{21}, s_{22}]$  whose vectorial coefficients can be calculated either using the integral in (1.13) or by eye inspection. With these vectorial coefficients, it is now possible to construct the signal space diagram as shown in Fig. 3.3.

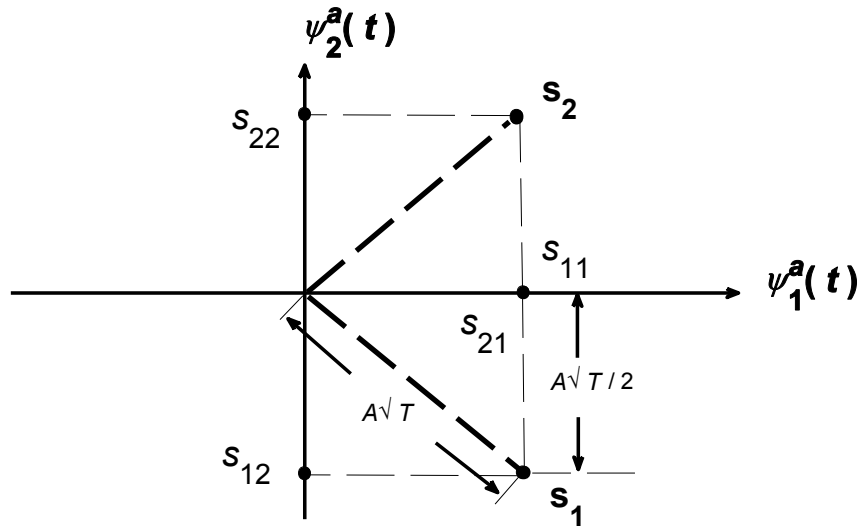


Fig. 3.3 Signal space diagram for  $s_1(t)$  and  $s_2(t)$  of Fig. 3.2.

As seen from Fig. 3.3. the two signal vectors are placed at  $90^\circ$  with respect to each other which is not surprising since  $s_1(t)$  and  $s_2(t)$  are orthogonal to each other. Additionally the angles  $s_1(t)$  and  $s_2(t)$  make with  $\psi_1^a(t)$  is  $45^\circ$ , since  $|s_{11}| = |s_{12}| = A\sqrt{T/2}$ ,  $|s_{21}| = |s_{22}| = A\sqrt{T/2}$ . Furthermore, the energies in  $s_1(t)$  and  $s_2(t)$  can be calculated from the lengths of  $\mathbf{s}_1$  and  $\mathbf{s}_2$  as well as from the time waveforms as shown in (3.5). Of course in both cases we arrive at identical results.

$$\begin{aligned} \varepsilon_1 &= \|\mathbf{s}_1\|^2 = s_{11}^2 + s_{12}^2 = \int_{-\infty}^{\infty} s_1^2(t) dt = A^2T \\ \varepsilon_2 &= \|\mathbf{s}_2\|^2 = s_{21}^2 + s_{22}^2 = \int_{-\infty}^{\infty} s_2^2(t) dt = A^2T, \quad \varepsilon_1 = \varepsilon_2 = \varepsilon_s \end{aligned} \quad (3.5)$$

**Exercise 3.1 :** Find  $s_1(t)$  and  $s_2(t)$  in terms of  $\psi_1(t)$  and  $\psi_2(t)$ , draw the related signal space diagram, signal vectors, energies and compare your results with the case of  $\psi_1^a(t)$  and  $\psi_2^a(t)$  and comment on them.

$s_1(t)$  and  $s_2(t)$  time waveforms of Fig. 3.2 and the associated signal space diagram in Fig. 3.3. constitute what is called PSK, since here the energies of signals (thus the length of signal vectors) are the same (denoted commonly as  $\varepsilon_s$ ) and the only differentiating factor is the respective angular location corresponding to phases in  $s_1(t)$  and  $s_2(t)$ . Looking at Fig. 3.3, we see that the two dimensional signal space is not used efficiently and we can place two more signals, namely  $s_3(t)$  and  $s_4(t)$  such that  $s_1(t) = -s_3(t)$  and  $s_4(t) = -s_2(t)$ , hence the vectors  $\mathbf{s}_3$  and  $\mathbf{s}_4$  will have a rotation of  $180^\circ$  with respect to  $\mathbf{s}_1$  and  $\mathbf{s}_2$ . The new signal space diagram comprising  $\mathbf{s}_1, \mathbf{s}_2, \mathbf{s}_3$  and  $\mathbf{s}_4$  is given in Fig. 3.4. Note that here we have reverted from  $\psi_1^a(t)$  and  $\psi_2^a(t)$  to  $\psi_1(t)$  and  $\psi_2(t)$ .

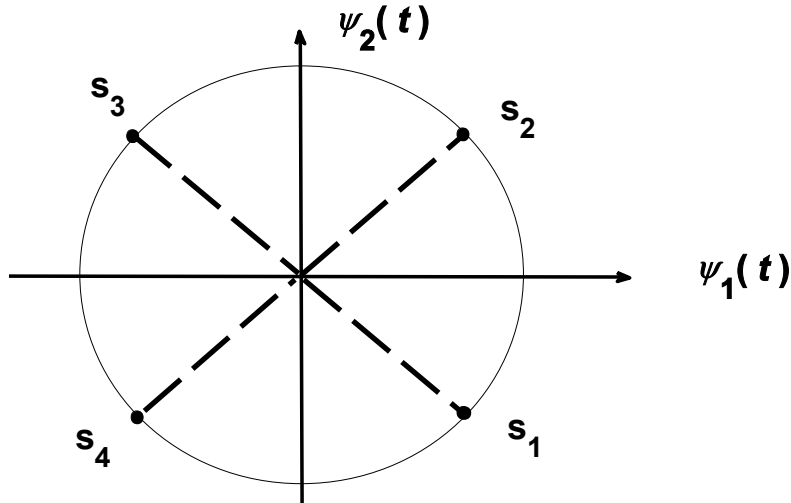


Fig. 3.4 Signal space diagram for 4 PSK signals  $s_1(t) \cdots s_4(t)$ .

In Fig. 3.4,  $M = 4$  (corresponding to 4 level signalling), this PSK scheme is also known as quadrature PSK. In the signal space diagram of Fig. 3.3, we had  $M = 2$  (binary). Since in PSK, all signal vectors are of same length (and same energies), it is customary to draw a circle passing through signal end points as indicated in Fig. 3.4. It is of course possible to add more signals to the two dimensional signal space of PSK. For instance, the case of  $M = 8$  is shown in Fig. 3.5 where we have removed the connections of signal vector ends to the origin for clarity. It is also possible to go to higher  $M$  values. This way, the appearance in the signal space diagrams will turn more into a constellation of stars. For this reason, signal space diagram is also called constellation diagram. For a general  $M$ , the  $m$ th signal waveform  $s_m(t)$  and signal vector  $\mathbf{s}_m$  from the signal set of  $s_1(t) \cdots s_m(t) \cdots s_M(t)$  can be formulated as

$$\begin{aligned}
 s_m(t) &= A\sqrt{T} [C_c \psi_1(t) + C_s \psi_2(t)] \quad , \quad C_c = \cos[2\pi(m-1)/M] \quad , \quad C_s = \sin[2\pi(m-1)/M] \\
 \psi_1(t) &= \begin{cases} \sqrt{2/T} & \text{for } 0 \leq t \leq T/2 \\ 0 & \text{elsewhere} \end{cases} \quad \psi_2(t) = \begin{cases} \sqrt{2/T} & \text{for } T/2 \leq t \leq T \\ 0 & \text{elsewhere} \end{cases} \\
 \mathbf{s}_m &= \{A\sqrt{T} \cos[2\pi(m-1)/M] \quad , \quad A\sqrt{T} \sin[2\pi(m-1)/M]\} \quad , \quad m = 1 \cdots M \quad (3.6)
 \end{aligned}$$

Note that the orthonormalized basis functions defined in (3.6) are the same as  $\psi_1^a(t)$  and  $\psi_2^a(t)$  of Fig. 3.1.



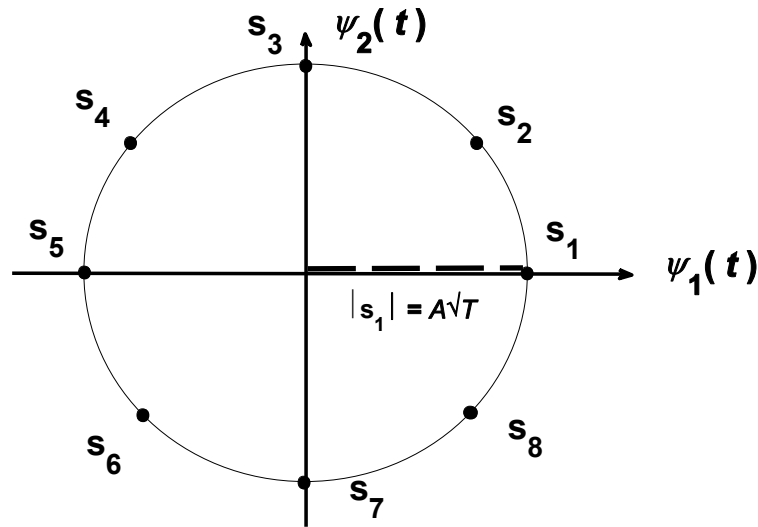


Fig. 3.5 Signal space diagram for 8 PSK signals  $s_1(t) \cdots s_8(t)$ .

**Exercise 3.2 :** From (3.6) write for the time signals of  $s_1(t) \cdots s_8(t)$ , signal vectors of  $\mathbf{s}_1 \cdots \mathbf{s}_8$  and see if they agree with the signal constellation of Fig. 3.5. Find the length and the energies of the signal vectors  $\mathbf{s}_1 \cdots \mathbf{s}_8$ .

As an alternative to time sliced version of representing the signal vectors, we can use the complex plane for PSK (and also QAM) constellation such that the positions of signal vectors are represented on a complex plane, since a complex plane is two dimensional as well. With this arrangement,  $\psi_1(t)$  will be replaced by the real part of the complex exponential and  $\psi_2(t)$  will be replaced by the imaginary part of the same exponential. Thus the signal vector  $\mathbf{s}_m$  of  $M$  ary PSK will become

$$\mathbf{s}_m = \left\{ A\sqrt{T} \exp[2\pi j(m-1)/M] \right\}, \quad m = 1 \cdots M \quad (3.7)$$

It is worthwhile to note that Matlab uses the notation expressed in (3.7).

It is easy to see that even with increasing  $M$ , the two dimensional signal space is still not efficiently used. One solution would be to create energy variations as well as phase variations in signal vectors, this way achieve a combination of ASK plus PSK. This combination will be called Quadrature Amplitude Modulation (QAM). An example of 16 QAM is shown in Fig. 3.6. As seen here, QAM constellations are usually arranged in the form of rectangles, although from probability of error view point, this is not the best placement of signal vectors, there is little difference between the rectangular arrangements and the optimum ones. Fig. 3.6 proves that QAM is indeed a combination of ASK and PSK. For instance, in the given constellation of Fig. 3.6, the collection of signal vectors  $\mathbf{s}_7, \mathbf{s}_6, \mathbf{s}_3$  and  $\mathbf{s}_2$  constitute 4 ASK, whereas the collection  $\mathbf{s}_4, \mathbf{s}_5, \mathbf{s}_{10}$  and  $\mathbf{s}_{15}$  represents 4 PSK. It is equally possible to identify other similar groupings.

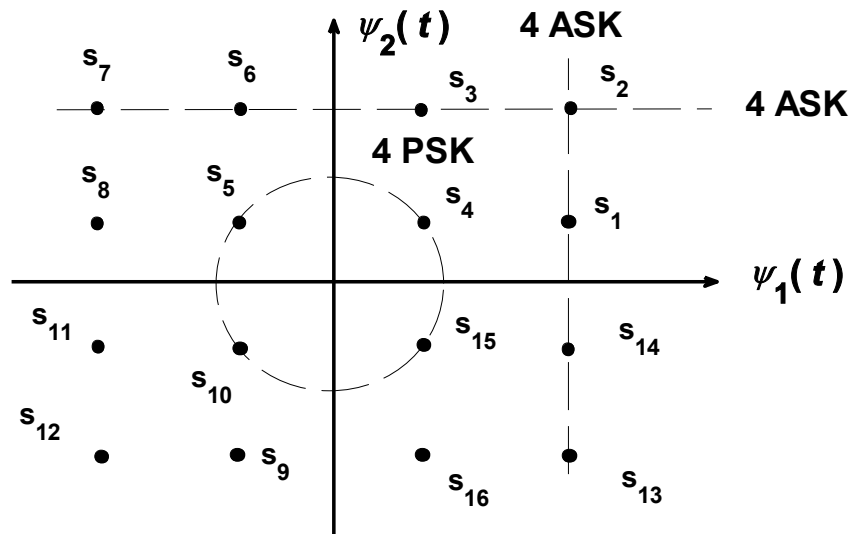


Fig. 3.6 Rectangular signal constellation for 16 QAM signals.

Arrangements other than the rectangular type are also possible in QAM. For instance placing of signal vectors on different circles within each other is another option as illustrated in Fig. 3.7. Of course, the objective here is to find the constellation (distribution of signal vectors) that will give the maximum distances between vector ends for the same total or average energy, since it is this criteria which will determine the probability of error performance.

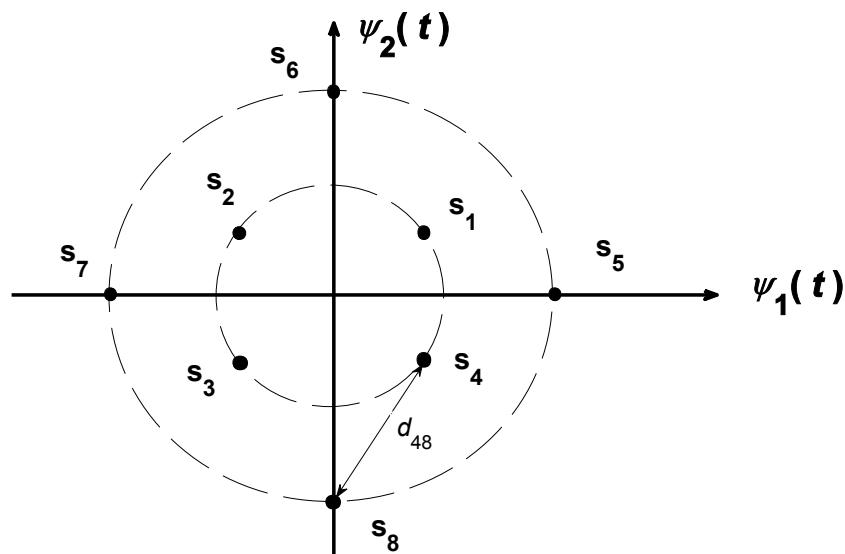


Fig. 3.7 Circular signal constellation for 8 QAM signals.

In practice QAM is used mostly in radio links.

## 4. Multidimensional Signals

### 4.1 Frequency Shift Keying (FSK)

With the context of multidimensional signals, here we will initially study Frequency Shift Keying (FSK). Although the other modulation types can be represented both in baseband (without carrier) and

bandpass (with carriers), FSK can only be written in terms of sinusoidal carriers. Assume that we choose  $M = 2$  and assign frequencies  $f_1$  and  $f_2$  to our message signals of  $s_1(t)$  and  $s_2(t)$ , then

$$\begin{aligned} s_1(t) &= \sqrt{2}A \cos(2\pi f_1 t) \quad , \quad 0 \leq t \leq T_b \quad , \quad T_b : \text{ Binary waveform duration} \\ s_2(t) &= \sqrt{2}A \cos(2\pi f_2 t) \quad , \quad 0 \leq t \leq T_b \quad , \quad \varepsilon_b = \int_0^{T_b} s_1^2(t) dt = \int_0^{T_b} s_2^2(t) dt = A^2 T_b \end{aligned} \quad (4.1)$$

Note that in the writing of signal waveforms, we have used slightly different notation than ASK and PSK. By setting  $\Delta f = f_m - f_{m-1}$ , adopting a starting frequency of  $f_c$  such that  $f_m = f_c + (m-1)\Delta f$  we can write for the  $m$ th signal as follows

$$\begin{aligned} s_m(t) &= \sqrt{2}A \cos[2\pi f_c t + 2\pi \Delta f (m-1)t] \quad , \quad 0 \leq t \leq T \\ \varepsilon_s &= \int_0^T s_m^2(t) dt = A^2 T = k\varepsilon_b = \varepsilon_b \log_2 M \quad , \quad m = 1 \cdots M \quad , \quad T = kT_b \end{aligned} \quad (4.2)$$

It is interesting to examine the variation of  $\Delta f$  (frequency separation) against  $T$  (symbol duration). To this end we define the correlation coefficient  $\gamma_{mn}$  as follows

$$\begin{aligned} \gamma_{mn} &= \frac{1}{\varepsilon_s} \int_0^T s_m(t) s_n(t) dt \\ &= \frac{1}{\varepsilon_s} \int_0^T 2A^2 \cos[2\pi f_c t + 2\pi \Delta f (m-1)t] \cos[2\pi f_c t + 2\pi \Delta f (n-1)t] dt \\ &= \frac{1}{T} \int_0^T \cos[2\pi f_c t + 2\pi \Delta f (m-n)t] dt + \frac{1}{T} \int_0^T \cos[2\pi f_c t + 2\pi \Delta f (m+n-2)t] dt \\ &\approx \frac{\sin[2\pi \Delta f (m-n)T]}{2\pi \Delta f (m-n)T} \end{aligned} \quad (4.3)$$

where on the second line, we have substitutions from (4.1) and the approximation on the line is due to  $f_c \gg 1/T$ . A plot of  $\gamma_{mn}$  against  $\Delta f$  is given in Fig. 4.1. As seen from this figure,  $\gamma_{mn}$  passes through zero at integer multiples of  $1/2T$ . It means at this values of  $\Delta f$ , the signals  $s_m(t)$  and  $s_n(t)$  are orthogonal. The minimum value of  $\gamma_{mn}$  is  $-0.217$  and reached at  $\Delta f = 0.715/T$ . These markings are important and form the basis of Orthogonal Frequency Division Multiplexing (OFDM), and minimum shift keying (MSK).

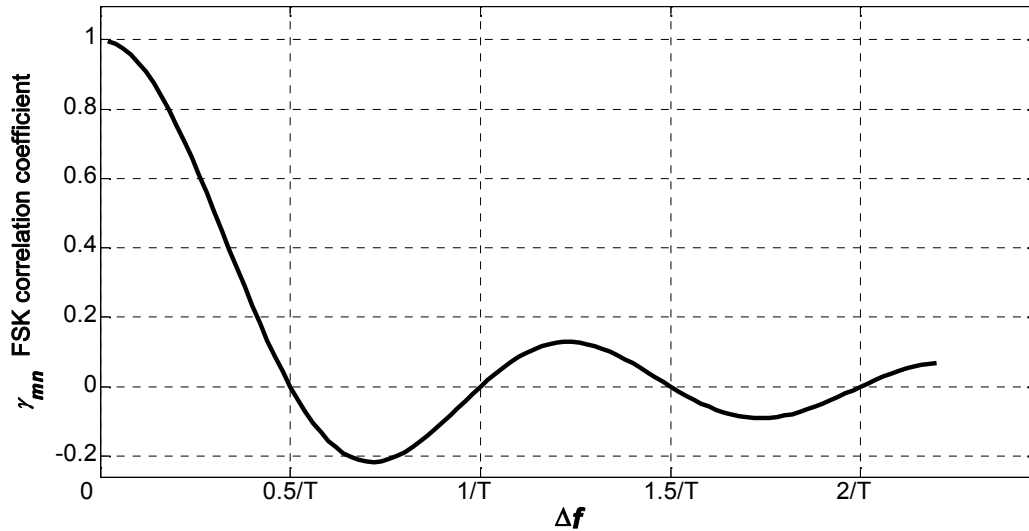
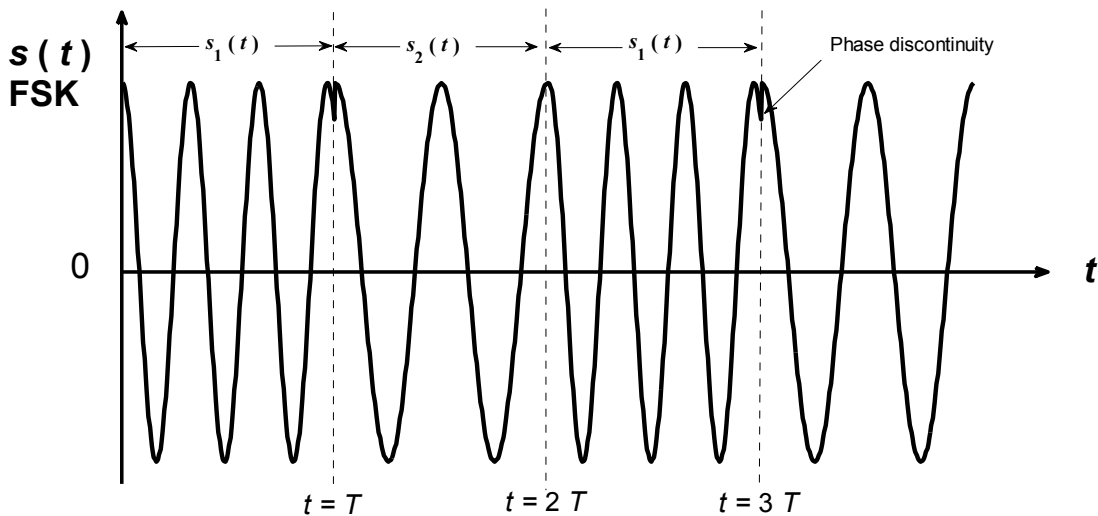


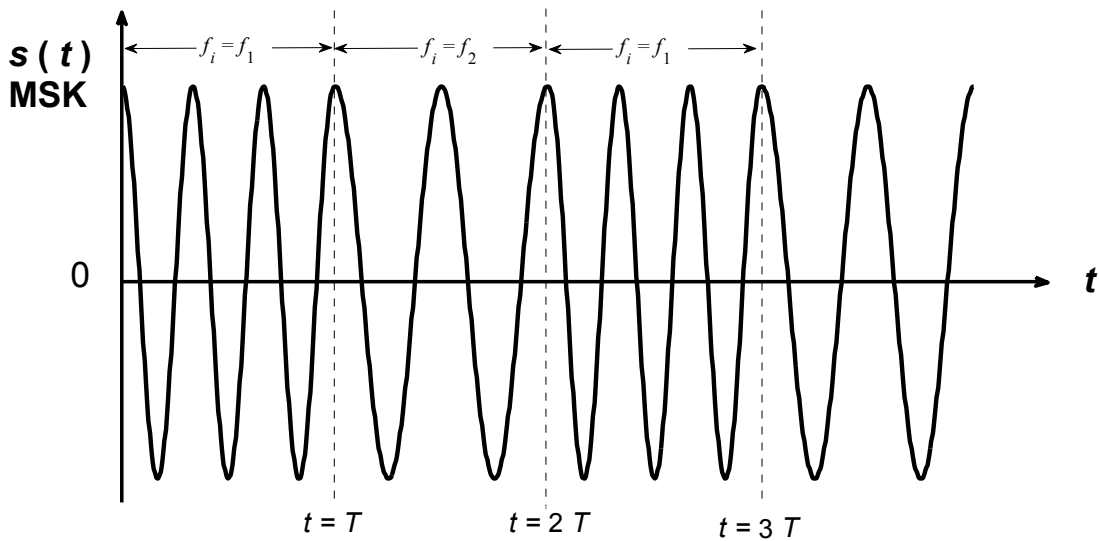
Fig. 4.1 The variation of FSK correlation coefficient  $\gamma_{mn}$  against  $\Delta f$ .

**Exercise 4.1 :** Write the mathematical expressions for FSK time signals and signal vectors for  $M = 8$ .

A typical binary FSK waveform is shown in Fig. 4.2a. It is interesting to observe in Fig. 4.2 that a phase discontinuity exists at the transitions from  $s_1(t)$  to  $s_2(t)$ . Phase discontinuities cause in more bandwidth requirements. Such transitions are eliminated in a modulation scheme called minimum shift keying (MSK). A sample of MSK is also illustrated in Fig. 4.2.b.



a) FSK signal with phase discontinuity.



b) MSK signal (without phase discontinuity)

Fig. 4.2 FSK and MSK signals illustrating the existence and the absence of phase discontinuity.

#### 4.2 Orthogonal Signal Waveforms and Pulse Position Modulation (PPM)

Orthogonal signal waveforms  $s_1^w(t) \dots s_4^w(t)$  and pulse position modulation signal waveforms  $s_1^p(t) \dots s_4^p(t)$  are shown in Fig. 4.3.

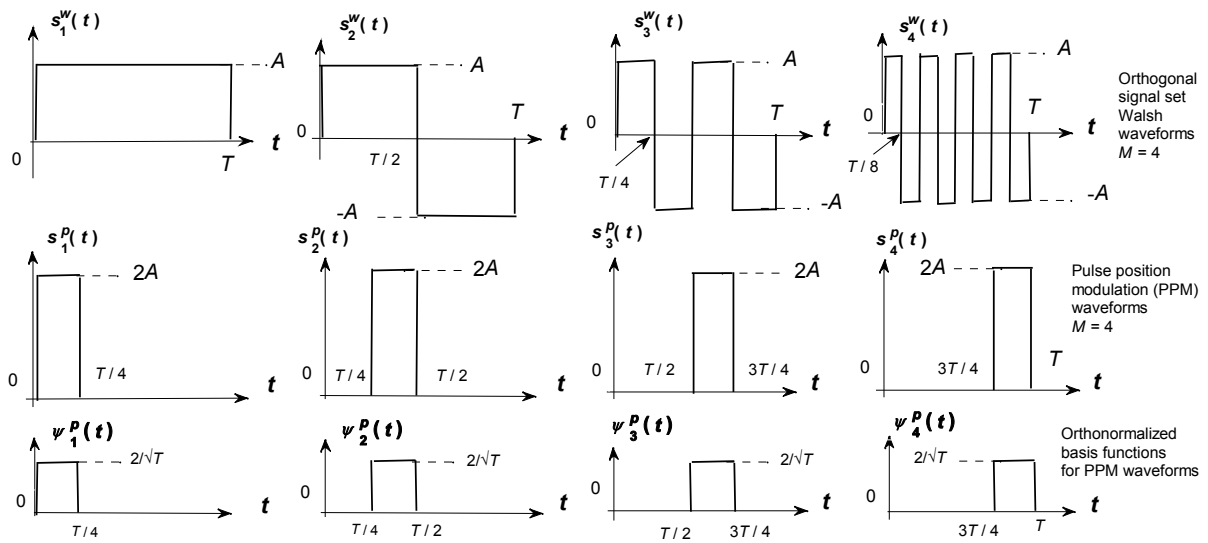


Fig. 4.3 Orthogonal signal waveform set (Walsh waveforms), pulse position modulation (PPM) waveforms and the orthonormalized basis functions for PPM waveforms.

The orthogonal waveforms displayed on the first row of Fig. 4.3 are derived from Walsh sequences and hence named as such. In both cases of Fig. 4.3,  $M = N = 4$ , that is the number of signals in the signal set is equivalent to the number of dimensions of the set. Therefore, we obviously need four orthonormalized basis functions to represent  $s_1^w(t) \dots s_4^w(t)$  and  $s_1^p(t) \dots s_4^p(t)$ . Those for the PPM

set are given on the last row of Fig. 4.3. Hence the PPM waveforms themselves, their time waveform and vectorial representation in terms of this basis functions  $\psi_1^p(t) \cdots \psi_4^p(t)$  can be written as follows

$$\begin{aligned}
 s_1^p(t) &= \begin{cases} 2A & 0 \leq t \leq T/4 \\ 0 & \text{otherwise} \end{cases} & s_2^p(t) &= \begin{cases} 2A & T/4 \leq t \leq T/2 \\ 0 & \text{otherwise} \end{cases} \\
 s_3^p(t) &= \begin{cases} 2A & T/2 \leq t \leq 3T/4 \\ 0 & \text{otherwise} \end{cases} & s_4^p(t) &= \begin{cases} 2A & 3T/4 \leq t \leq T \\ 0 & \text{otherwise} \end{cases} \\
 \psi_1^p(t) &= \begin{cases} 2/\sqrt{T} & 0 \leq t \leq T/4 \\ 0 & \text{otherwise} \end{cases} & \psi_2^p(t) &= \begin{cases} 2/\sqrt{T} & T/4 \leq t \leq T/2 \\ 0 & \text{otherwise} \end{cases} \\
 \psi_3^p(t) &= \begin{cases} 2/\sqrt{T} & T/2 \leq t \leq 3T/4 \\ 0 & \text{otherwise} \end{cases} & \psi_4^p(t) &= \begin{cases} 2/\sqrt{T} & 3T/4 \leq t \leq T \\ 0 & \text{otherwise} \end{cases} \\
 s_1^p(t) &= A\sqrt{T}\psi_1^p(t), \quad s_2^p(t) = A\sqrt{T}\psi_2^p(t), \quad s_3^p(t) = A\sqrt{T}\psi_3^p(t), \quad s_4^p(t) = A\sqrt{T}\psi_4^p(t) \\
 \mathbf{s}_1^p &= [s_{11}^p, s_{12}^p, s_{13}^p, s_{14}^p] = [A\sqrt{T}, 0, 0, 0], \quad \mathbf{s}_2^p = [s_{21}^p, s_{22}^p, s_{23}^p, s_{24}^p] = [0, A\sqrt{T}, 0, 0] \\
 \mathbf{s}_3^p &= [s_{31}^p, s_{32}^p, s_{33}^p, s_{34}^p] = [0, 0, A\sqrt{T}, 0], \quad \mathbf{s}_4^p = [s_{41}^p, s_{42}^p, s_{43}^p, s_{44}^p] = [0, 0, 0, A\sqrt{T}] \quad (4.4)
 \end{aligned}$$

It is clear from Fig. 4.3 and the expressions in (4.4) that as we go to higher dimensions, we slice the time axis more, this in turn increases our bandwidth requirement, So we can establish the following relation

$$\text{Number of dimensions } N \uparrow \quad \text{Bandwidth } \uparrow \quad (4.5)$$

**Exercise 4.2 :** Find the orthonormal basis functions of  $s_1^w(t) \cdots s_4^w(t)$ , i.e.  $\psi_1^w(t) \cdots \psi_4^w(t)$  either by hand or by eye inspection or by using ECE376\_GSOrthogonalWaveforms\_Exp4.m and express  $s_1^w(t) \cdots s_4^w(t)$  in terms of  $\psi_1^w(t) \cdots \psi_4^w(t)$  like done in (4.4). Find the vectorial representation of  $s_1^w(t) \cdots s_4^w(t)$  and the energies in each signal.

From the above analysis, we summarize our findings as follows

- ASK is one dimensional ( $N = 1$ ), PSK and QAM are two dimensional ( $N = 2$ ), whereas FSK can be multidimensional ( $N > 2$ ).
- ASK signals differ by energies. There is only angular variation but no energy variation in the PSK signals. In QAM, there is energy as well as angular variations in QAM signals.
- For the same symbol rate, i.e., same symbol duration of  $T$ , Bandwidth of ASK < Bandwidth of PSK and QAM.
- As the dimensionality, i.e.,  $N$  increases, bandwidth requirement increases as well.

## 5. Detection of Signal in Presence of Additive White Gaussian Noise – Correlators and Matched Filters

We assume that within a time interval of  $0 \leq t \leq T$ , our transmitter randomly sends one of the  $s_1(t) \cdots s_M(t)$  signals, namely  $s_m(t)$  and in the communication channel, only additive white Gaussian noise (AWGN) is added to the signal, so that the received signal  $r(t)$  is

$$r(t) = s_m(t) + n(t) \quad , \quad S_n(f) = \frac{N_0}{2} = \sigma_n^2 \quad (5.1)$$

where  $S_n(f)$  is known as noise spectral density function,  $N_0$  and  $\sigma_n^2$  are noise spectral density level and noise variance. It is obvious that  $S_n(f)$  is independent of frequency  $f$ , hence the White nature of Gaussian noise.

Such a channel model is known as (band unlimited) AWGN channel and depicted in Fig. 5.1. It is clear that in this channel, there is no band limitation, which means that

$$C(f) = 1 \quad , \quad c(t) = \delta(t) \quad , \quad \delta(t) : \text{Time delta function} \quad (5.2)$$

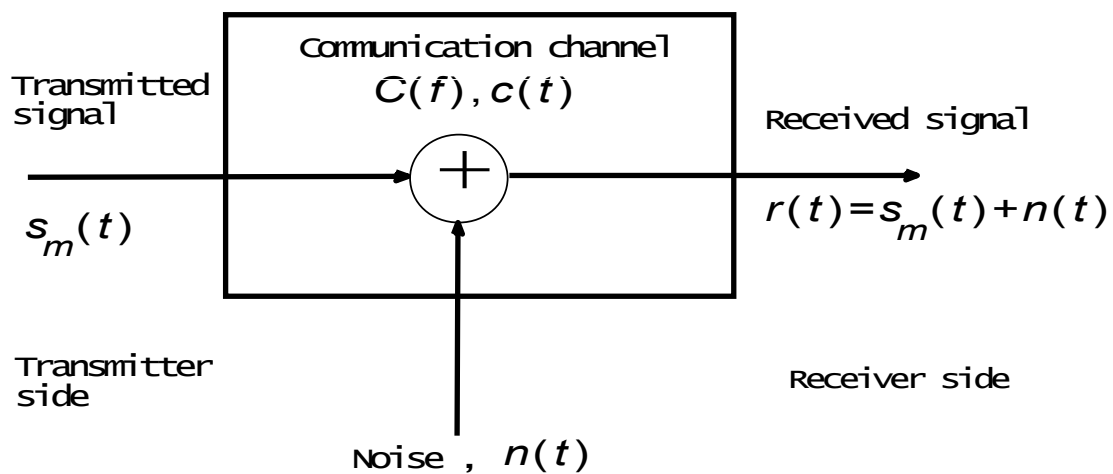


Fig. 5.1 AWGN channel model.

The receiver has a knowledge of modulation type and symbol duration,  $T$  that are employed at the transmitter. Furthermore the receiver also knows the set of signals  $s_1(t) \cdots s_M(t)$ , i.e. the alphabet used by the transmitter. Finally we assume that the receiver is able to extract the beginning of time interval  $0 \leq t \leq T$ , called synchronization. So the job of the receiver is to demodulate the incoming signal  $r(t)$  and decide correctly which  $s_m(t)$  was sent from the transmitter within the time interval  $0 \leq t \leq T$ . Note that since we are dealing with an unlimited channel, it is sufficient to consider any symbol interval. Here we choose, the interval,  $0 \leq t \leq T$ . To perform demodulation tasks, we pass the received signal through a correlator as shown in Fig. 5.2. Basically the operations performed in the correlator of Fig. 5.2 are feeding the received signal simultaneously to  $N$  branches, multiplying the received signal  $r(t)$  on each branch by one of the orthonormal basis functions  $\psi_1(t) \cdots \psi_N(t)$  (the same ones used at transmitter to construct the signal  $s_m(t)$ ), integrating the resultant over one

symbol duration, and sampling at the end of this duration, forming the vector array  $\mathbf{r}$  by collecting the individual components  $r_1 \cdots r_N$ , eventually sending  $\mathbf{r}$  to a detector to decide which  $s_m(t)$  was sent from the transmitter. The operations carried out on the  $n$ th branch of this correlator can mathematically be described as

$$\int_0^T r(t) \psi_n(t) dt = \int_0^T [s_m(t) + n(t)] \psi_n(t) dt$$

$$r_n = s_{mn} + n_n \quad n = 1 \cdots N$$

$$s_{mn} = \int_0^T s_m(t) \psi_n(t) dt, \quad n_n = \int_0^T n(t) \psi_n(t) dt \quad (5.3)$$

Note that the definition of  $s_{mn}$  is equivalent to the one in (1.13).

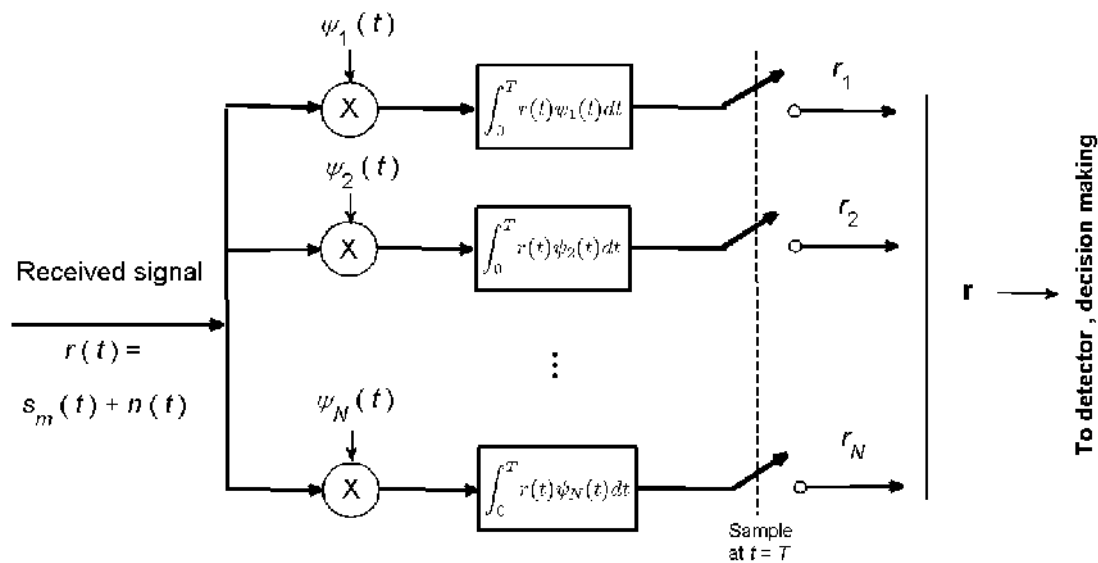


Fig. 5.2 Correlator type of demodulator.

Considering all branches in the correlator of Fig. 5.2, we get

$$\mathbf{r} = \mathbf{s}_m + \mathbf{n} \quad (5.4)$$

(5.4) means the totality of the operations in the correlator can be treated as row arrays of  $\mathbf{r}$ ,  $\mathbf{s}_m$  and  $\mathbf{n}$ , where

$$\mathbf{r} = [r_1 \cdots r_n \cdots r_N], \quad \mathbf{s}_m = [s_{m1} \cdots s_{mn} \cdots s_{mN}], \quad \mathbf{n} = [n_1 \cdots n_n \cdots n_N] \quad (5.5)$$

It is important to point out that  $\mathbf{s}_m$  is deterministic in the sense that it will take upon one of the values from the set  $\mathbf{s}_1 \cdots \mathbf{s}_M$ , while  $\mathbf{n}$  is random. The probability density function (pdf) for the amplitude distribution of one  $n_n$  sample of  $\mathbf{n}$  is the same as input noise, hence

$$f(n_n) = \frac{1}{(\pi N_0)^{0.5}} \exp\left(-\frac{n_n^2}{N_0}\right), \quad N_0 = 2\sigma_n^2, \quad n = 1 \cdots N \quad (5.6)$$



where  $N_0/2$  is the noise spectral density and  $\sigma_n^2$  is the variance. All  $n_n$  samples have zero mean and are uncorrelated, which means

$$\begin{aligned}
 E[n_n] &= \int_0^T E[n(t)] \psi_n(t) dt = 0 \\
 E[n_n n_m] &= \int_0^T \int_0^T E[n(t)n(\tau)] \psi_n(t) \psi_m(\tau) dt d\tau \\
 &= \int_0^T \int_0^T \frac{N_0}{2} \delta(t-\tau) \psi_n(t) \psi_m(\tau) dt \\
 &= \frac{N_0}{2} \int_0^T \psi_n(t) \psi_m(t) dt \\
 &= \frac{N_0}{2} \delta_{mn} \quad , \quad \delta_{mn} = 0 \text{ if } n \neq m \quad , \quad \delta_{mn} = 1 \text{ if } n = m
 \end{aligned} \tag{5.7}$$

As a consequence of (5.5) and (5.6)

$$\begin{aligned}
 f(\mathbf{n}) &= \prod_{n=1}^N f(n_n) = \frac{1}{(\pi N_0)^{N/2}} \exp\left(-\sum_{n=1}^N \frac{n_n^2}{N_0}\right) \\
 E[r_n] &= E[s_{mn} + n_n] = E[s_{mn}] + E[n_n] = s_{mn} + 0 = s_{mn} \\
 f(\mathbf{r} | \mathbf{s}_m) &= \prod_{n=1}^N f(r_n | s_{mn}) \quad , \quad m = 1 \dots M \\
 f(r_n | s_{mn}) &= \frac{1}{(\pi N_0)^{0.5}} \exp\left[-(r_n - s_{mn})^2 / N_0\right] \quad , \quad n = 1 \dots N \\
 f(\mathbf{r} | \mathbf{s}_m) &= \frac{1}{(\pi N_0)^{N/2}} \exp\left[-\sum_{n=1}^N \frac{(r_n - s_{mn})^2}{N_0}\right] \\
 &= \frac{1}{(\pi N_0)^{N/2}} \exp\left[-\frac{\|\mathbf{r} - \mathbf{s}_m\|^2}{N_0}\right] \quad , \quad m = 1 \dots M
 \end{aligned} \tag{5.8}$$

The development in (5.8) means that (vectorwise) when noise  $\mathbf{n}$  is added to the incoming signal  $\mathbf{s}_m$ , then the received signal  $\mathbf{r}$  becomes a Gaussian random variable as well. This way the received signal inherits all properties of noise, except that the previous zero mean is now shifted to  $\mathbf{s}_m$ . In a way, this is like adding a DC shift ( $\mathbf{s}_m$ ) to an AC signal  $\mathbf{n}$ . Note that in (5.5) noise vector  $\mathbf{n}$  is shown to be  $N$  dimensional. This is because the correlator of Fig. 5.2 takes the projections of noise signal  $n(t)$  onto an  $N$  dimensional space. Prior to such an operation, noise signal  $n(t)$  (i.e. the noise in nature) has infinite number of dimensions.

It is also possible to perform the demodulation via match filter type of demodulator. This is shown in Fig. 5.3. As seen in Fig. 5.3, the previous acts of multiplying the received signal by orthonormal basis functions and the integrating the resulting product are concentrated in the boxes known as matched filters (MFs). This can be proven mathematically by writing the output from MF  $n$  th branch on the as follows.

$$\begin{aligned}
 y_n(t) &= \int_0^t r(\tau) h_n(t-\tau) d\tau \\
 &= \int_0^t r(\tau) \psi_n(T-t+\tau) d\tau, \quad n=1 \dots N
 \end{aligned}
 \tag{5.9}$$

After sampling at  $t = T$ , we obtain

$$y_n(T) = \int_0^T r(\tau) \psi_n(\tau) d\tau, \quad n=1 \dots N
 \tag{5.10}$$

(5.10) will deliver the same result as the first line of the integral in (5.3).

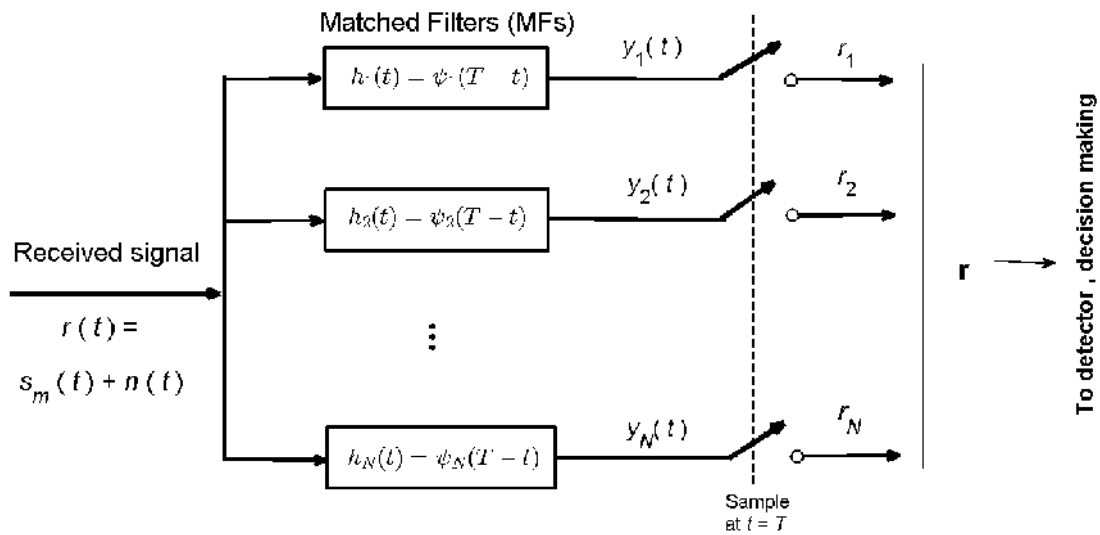
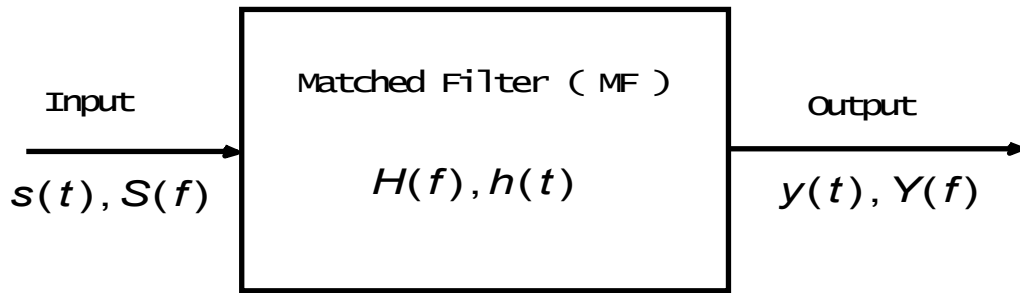


Fig. 5.3 Matched Filter (MF) type of demodulator.

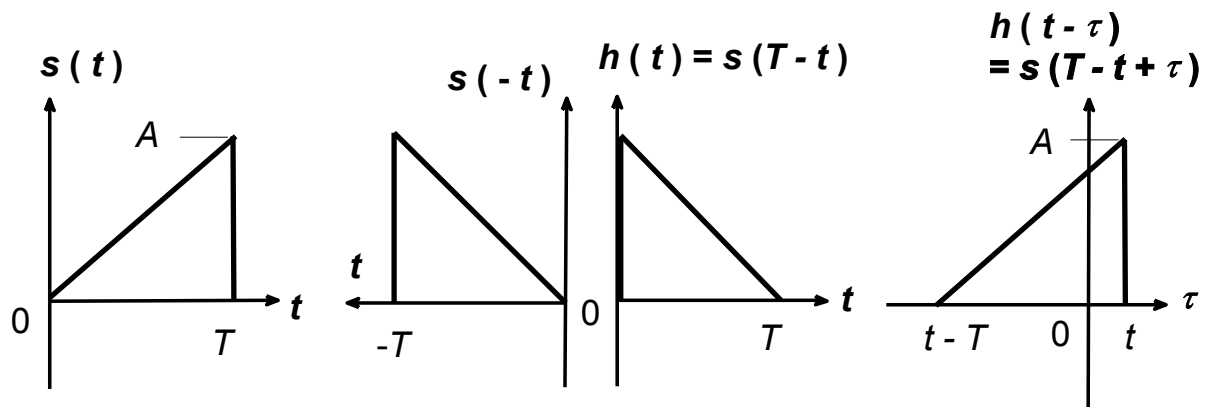
It is instructive to examine the time domain properties of MF. The impulse response of a filter matched to an input signal of  $s(t)$  is given by  $h(t) = s(T-t)$ . Then the response from such a filter would be

$$y(t) = \int_0^t s(\tau) h(t-\tau) d\tau = \int_0^t s(\tau) s(T-t+\tau) d\tau
 \tag{5.11}$$

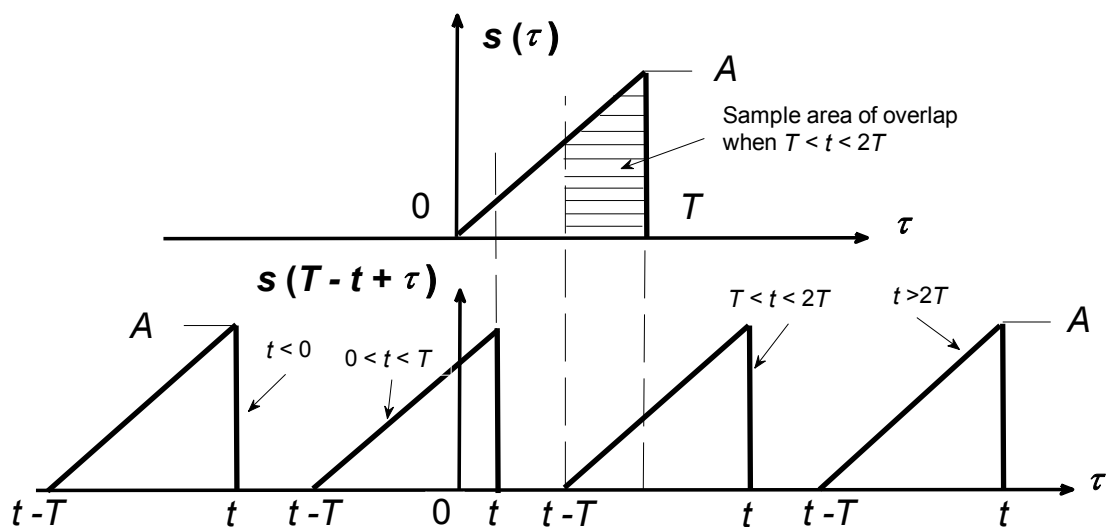
So the output from the matched filter can be interpreted as the time autocorrelation function of the input signal  $s(t)$ . An example input and output of MF are given in Fig. 5.4. As seen from Fig. 5.4c, the match filter response inside the convolution integral becomes oriented in the same direction as the input so that maximum similarity (correlation) is established at the output at the instance of  $t = T$ .



a) Block diagram of matched filter (MF)



b) Orientation of input signal to matched filter (MF)



c) Output from matched filter (MF) via convolution

Fig. 5.4 Block diagram, orientation of input signal and obtaining output signal from MF via convolution.

To find the output of MF for the input given in Fig. 5.4, we need the mathematical expressions of  $s(\tau)$  and  $s(T-t+\tau)$  as seen for the integration in (5.11). These are

$$s(\tau) = A \frac{\tau}{T}, \quad s(T-t+\tau) = -A \frac{t-\tau}{T} + A \quad (5.12)$$

Again looking at Fig. 5.4 c), we identify four different regions of integration for the expression of (5.11) which are

$$y(t) = \begin{cases} y_1(t) = 0 & t \leq 0 \\ y_2(t) = \int_0^t s(\tau) s(T-t+\tau) d\tau & 0 \leq t \leq T \\ y_3(t) = \int_{t-T}^T s(\tau) s(T-t+\tau) d\tau & T \leq t \leq 2T \\ y_4(t) = 0 & t \geq 2T \end{cases} \quad (5.13)$$

Note that on the first and last lines of (5.13), the result is zero because there is no overlap between  $s(\tau)$  and  $s(T-t+\tau)$ , while on the second and third lines, the integrand is the same as expected, but the integration limits are adjusted according to the areas of overlap. After using (5.12) in (5.13), we get

$$y(t) = \begin{cases} y_1(t) = 0 & t \leq 0 \\ y_2(t) = -\frac{A^2 t^3}{6T^2} + \frac{A^2 t^2}{2T} & 0 \leq t \leq T \\ y_3(t) = \frac{A^2}{6T^2} (t-T)^3 - \frac{A^2 t}{2} + \frac{5A^2 T}{6} & T \leq t \leq 2T \\ y_4(t) = 0 & t \geq 2T \end{cases} \quad (5.14)$$

For the results (meaning the second and third lines) in (5.14), the tests conducted at the check points  $t=0$ ,  $t=T$  and  $t=2T$  are given in (5.15). Note that these tests, of course, do not guarantee the absolute correctness of the formulations given for  $y_2(t)$  and  $y_3(t)$  in (5.14). We show the plot of  $y(t)$  in Fig. 5.5.

$$\begin{aligned}
y_2(t=0) &= -\frac{A^2(t=0)^3}{6T^2} + \frac{A^2(t=0)^2}{2T} = 0 && \text{Test for } t=0 : \text{OK} \\
y_2(t=T) &= -\frac{A^2(t=T)^3}{6T^2} + \frac{A^2(t=T)^2}{2T} = \frac{A^2T}{3} = \int_0^T s^2(t) dt = \varepsilon_s && \text{Test for } t=T : \text{OK} \\
y_3(t=T) &= \frac{A^2}{6T^2}(t=T-T)^3 - \frac{A^2(t=T)}{2} + \frac{5A^2T}{6} = \frac{A^2T}{3} = \varepsilon_s && \text{Test for } t=T : \text{OK} \\
y_3(t=2T) &= \frac{A^2}{6T^2}(t=2T-T)^3 - \frac{A^2(t=2T)}{2} + \frac{5A^2T}{6} = \frac{A^2T}{3} = 0 && \text{Test for } t=2T : \text{OK}
\end{aligned}$$

(5.15)

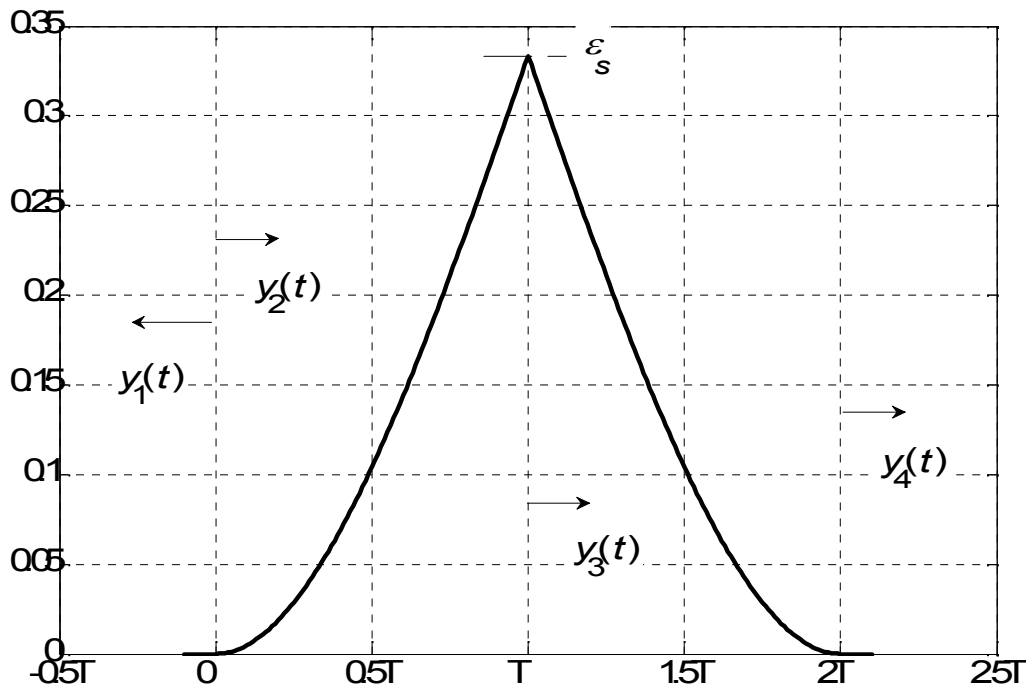


Fig. 5.5 The output from MF, when the input is as shown in Fig. 5.4.

As seen from Fig. 5.5, the peak of  $y(t)$  occurs at  $t = T$ . This explains also why we have chosen the sampling instance  $t = T$  for correlator in Fig. 5.2 and matched filter in Fig. 5.3. It is important to note that the output of MF comes out to be in units of energy, whereas we expect it to be in units of voltage (or current). To correct this, we have to divide the output of MF by the square root of energy of input.

Finally we examine the frequency domain interpretation of MF. To this end we assume that for a signal of  $s(t)$  the time response of matched filter is given by  $h(t) = s(T-t)$ , thus the Fourier transform of  $s(T-t)$  will be

$$\begin{aligned}
H(f) &= \int_0^T s(T-t) \exp(-2j\pi ft) dt \\
&= \left[ \int_0^T s(\tau) \exp(2j\pi f\tau) d\tau \right] \exp(-2j\pi fT) \\
&= S^*(f) \exp(-2j\pi fT)
\end{aligned} \tag{5.16}$$

The last line in (5.16) means that the frequency response of MF is equal to the multiplication of the complex conjugate of the frequency response of the input signal and phase factor  $\exp(-2j\pi fT)$ , representing the time delay of  $T$  in  $s(T-t)$ . The output from MF in will then be

$$\begin{aligned}
y(t) &= \int_{-\infty}^{\infty} Y(f) \exp(2j\pi ft) df \\
&= \int_{-\infty}^{\infty} |S(f)|^2 \exp(-2j\pi fT) \exp(2j\pi ft) df \\
y(t=T) &= \int_{-\infty}^{\infty} |S(f)|^2 df = \int_{-\infty}^{\infty} s^2(t) dt = \varepsilon_s
\end{aligned} \tag{5.17}$$

where on the last line we have taken into account the sampling at the instance of  $t = T$ . Then we have used Parseval's relation to establish the energy equivalence of a (time limited) signal along time and frequency axis. Since it is a bit awkward to find the output of MF in units of energy, usually we scale the response of MF by the square root of energy. Note that such a scaling is already accounted for in the orthonormalized functions of  $\psi_1(t) \cdots \psi_N(t)$ .

The last line of (5.17) gives the signal output as amplitude, thus its square will give the output power, that is

$$P_s = y^2(T) = \varepsilon_s^2 \tag{5.18}$$

The noise with a spectral density of  $S_n(f) = N_0/2$ , when fed to an MF whose frequency response is  $H(f) = S^*(f) \exp(-2j\pi fT)$  will deliver spectral density output of

$$S_0(f) = |H(f)|^2 S_n(f) = |S(f)|^2 N_0/2 \tag{5.19}$$

As a result, noise power at the output of MF will be

$$P_n = \int_{-\infty}^{\infty} S_0(f) df = \frac{N_0}{2} \int_{-\infty}^{\infty} |S(f)|^2 df = \frac{\varepsilon_s N_0}{2} \tag{5.20}$$

By using (5.18) and (5.20), we can calculate the signal to noise ratio (SNR) at the output as follows

$$\text{SNR} = \frac{P_s}{P_n} = \frac{\varepsilon_s^2}{\varepsilon_s N_0 / 2} = \frac{2\varepsilon_s}{N_0} \tag{5.21}$$

## 6. Optimum Detector

By optimum detector, we mean a detector that makes best use of the received (statistical) information and establishes a correct decision as far as possible. As seen from Figs. 5.2 and 5.3, the received to be used by the optimum detector is  $\mathbf{r} = [r_1; \dots; r_N]$ . From (5.8), we know that  $\mathbf{r}$  is a Gaussian random variable (a property inherited from noise) with a mean of  $\mathbf{s}_m$  (a property inherited from the transmitted signal). Vectorwise  $\mathbf{r} = \mathbf{s}_m + \mathbf{n}$ . So if the possible number of transmitted signals was  $M = 4$  and the dimensionality of the signal space was  $N = 3$ , then the appearance of the signal space diagram would be something like that shown in Fig. 6.1 assuming  $s_1(t)$  was transmitted. Here the cloud around each signalling point represents the spherical (since  $N = 3$ ) noise observed after many receptions. At a given instance of time received vector  $\mathbf{r}$  would be as shown.

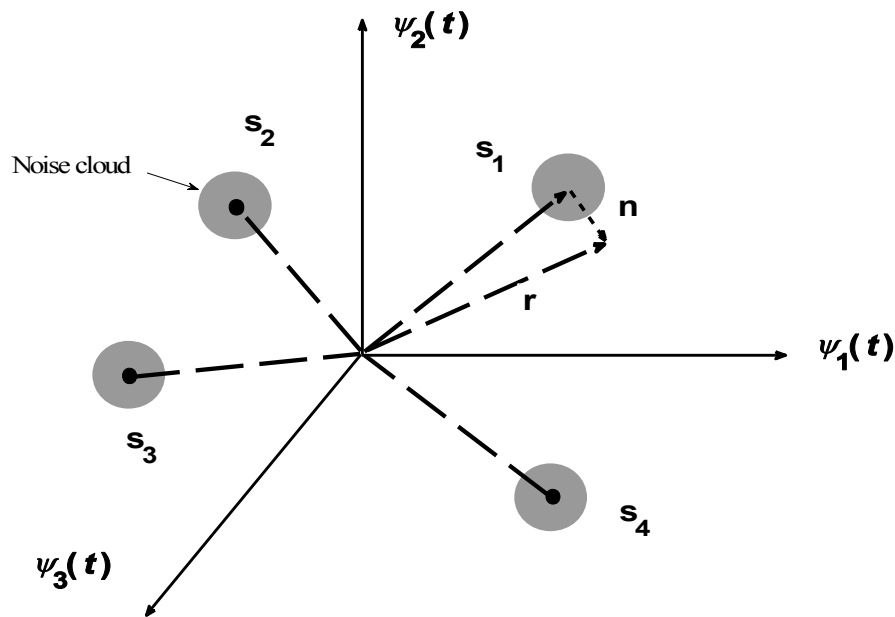


Fig. 6.1 The appearance of signal space after AWGN channel.

Now we aim for an optimum detector that will make a decision based on the computation of the posterior probability defined as

$$P(\text{signal } \mathbf{s}_m \text{ was transmitted} | \text{given received signal vector } \mathbf{r}) = P(\mathbf{s}_m | \mathbf{r}) \quad (6.1)$$

Our criteria will be to find  $m$  value that will maximize  $P(\mathbf{s}_m | \mathbf{r})$ , when  $m$  ranges in  $m = 1 \dots M$ . Upon finding the  $m$  value that has maximized  $P(\mathbf{s}_m | \mathbf{r})$ , we arrive at the decision that it is most likely that this particular  $\mathbf{s}_m$  was transmitted. So our optimum decision rule boils down to evaluating  $P(\mathbf{s}_m | \mathbf{r})$  and is named as maximum a posteriori probability (MAP) criterion.

Using Bayes rule, we can express  $P(\mathbf{s}_m | \mathbf{r})$  as

$$P(\mathbf{s}_m | \mathbf{r}) = \frac{f(\mathbf{r} | \mathbf{s}_m)P(\mathbf{s}_m)}{f(\mathbf{r})} \quad (6.2)$$

where  $f(\mathbf{r} | \mathbf{s}_m)$  is the conditional pdf of  $\mathbf{r}$  given that  $\mathbf{s}_m$  was transmitted.  $P(\mathbf{s}_m)$  is the probability that signal  $\mathbf{s}_m$  was transmitted.  $f(\mathbf{r})$  in the denominator of (6.2) is the pdf vector  $\mathbf{r}$  and will be given by the following sum

$$f(\mathbf{r}) = \sum_{m=1}^M f(\mathbf{r} | \mathbf{s}_m)P(\mathbf{s}_m) \quad (6.3)$$

We can take the formulation of  $f(\mathbf{r} | \mathbf{s}_m)$  from (5.8), but even then, it is not possible to arrive at a simplified expression of  $P(\mathbf{s}_m | \mathbf{r})$ , since individual probability of signal sent from the transmitter may be different. If however the transmitter sends all  $\mathbf{s}_m$  signals,  $m = 1 \dots M$  with equal probability, then

$$P(\mathbf{s}_m) = \frac{1}{M} \quad (6.4)$$

As a result

$$\text{Max}[P(\mathbf{s}_m | \mathbf{r})] = \text{Max} \left[ \frac{f(\mathbf{r} | \mathbf{s}_m)}{\sum_{m=1}^M f(\mathbf{r} | \mathbf{s}_m)} \right] \equiv \text{Max}[f(\mathbf{r} | \mathbf{s}_m)] \quad (6.5)$$

The reason that we have been able to write the last expression in (6.5) is that the sum in the denominator of the middle expression remains the same whichever  $m$  is selected. Therefore this sum has no role in the determination of  $\text{Max}[P(\mathbf{s}_m | \mathbf{r})]$ . So finding  $\text{Max}[P(\mathbf{s}_m | \mathbf{r})]$  is equivalent to finding  $\text{Max}[f(\mathbf{r} | \mathbf{s}_m)]$ , such a reduced decision strategy is called maximum likelihood (ML) criterion. From (5.8) we see that  $f(\mathbf{r} | \mathbf{s}_m)$  contains a Gaussian exponential, thus it may be easier to work with the  $\log_e$  (denoted by  $\ln$ ), hence

$$\text{Max} \left\{ \ln[f(\mathbf{r} | \mathbf{s}_m)] \right\} = \text{Max} \left[ \frac{-N}{2} \ln(\pi N_0) - \frac{1}{N_0} \sum_{n=1}^N (r_n - s_{mn})^2 \right] \quad (6.6)$$

We note that terms that do not contain the index  $m$  are irrelevant in the maximizing process, therefore, we take the last term in (6.6) and set it to a distance metrics,  $D(\mathbf{r}, \mathbf{s}_m)$

$$D(\mathbf{r}, \mathbf{s}_m) = \sum_{n=1}^N (r_n - s_{mn})^2 \quad (6.7)$$



Because of the minus sign in front of the sum in (6.6), seeking  $\text{Max}[P(\mathbf{s}_m | \mathbf{r})]$  will now be equivalent to  $\text{Min}[D(\mathbf{r}, \mathbf{s}_m)]$ . As the name implies and as also detected from (6.6), when the index  $m$  is run from 1 to  $M$ , the distance metrics  $D(\mathbf{r}, \mathbf{s}_m)$  will calculate one by one the distances of all signals that are likely to be sent from the transmitter to the received vector  $\mathbf{r}$ . In the end by selecting  $\text{Min}[D(\mathbf{r}, \mathbf{s}_1), D(\mathbf{r}, \mathbf{s}_2), \dots, D(\mathbf{r}, \mathbf{s}_M)]$ , we shall have arrived at the optimum decision based on MAP criterion. Such an operation is carried out for the sample constellation of Fig. 6.1 and illustrated in Fig. 6.2.

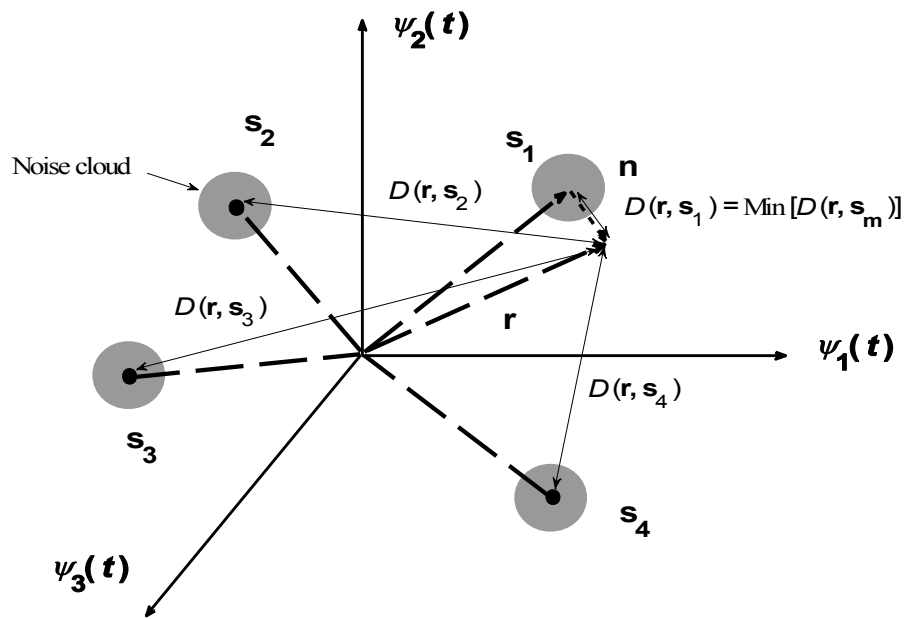


Fig. 6.2 Calculation of distance metrics for the sample constellation of Fig. 6.1.

As clearly seen from Fig. 6.2, this operation will definitely to the correct decision, so long as the noise  $\mathbf{n}$  added to  $\mathbf{s}_1$  (remember that we have already assumed that  $\mathbf{s}_1(t)$  was sent from the transmitter) is at the amplitude and angle as shown.

Expanding (6.7), we get

$$\begin{aligned}
 D(\mathbf{r}, \mathbf{s}_m) &= \sum_{n=1}^N r_n^2 - 2 \sum_{n=1}^N r_n s_{mn} + \sum_{n=1}^N s_{mn}^2 \\
 &= \|\mathbf{r}\|^2 - 2 \mathbf{r} \cdot \mathbf{s}_m + \|\mathbf{s}_m\|^2 \\
 D^a(\mathbf{r}, \mathbf{s}_m) &= -2 \mathbf{r} \cdot \mathbf{s}_m + \|\mathbf{s}_m\|^2, \quad C(\mathbf{r}, \mathbf{s}_m) = 2 \mathbf{r} \cdot \mathbf{s}_m - \|\mathbf{s}_m\|^2 \quad (6.8)
 \end{aligned}$$

On the second line of (6.8), we have reverted to vectorial notation, on the third line in the definition of  $D(\mathbf{r}, \mathbf{s}_m)$ , we have dropped  $\|\mathbf{r}\|^2$ , since it is common to all calculations of distance metrics, hence no effect on the result, thus have defined a new function called  $D^a(\mathbf{r}, \mathbf{s}_m)$ . Finally on the third line of (6.8) we have introduced correlation metrics  $C(\mathbf{r}, \mathbf{s}_m)$  which is the negative  $D^a(\mathbf{r}, \mathbf{s}_m)$ . Since in

the search of  $\text{Max}[P(\mathbf{s}_m|\mathbf{r})]$ , we opted to seek  $\text{Min}[D(\mathbf{r}, \mathbf{s}_m)]$  and  $C(\mathbf{r}, \mathbf{s}_m)$  is opposite sign to  $D(\mathbf{r}, \mathbf{s}_m)$  and consequently  $D^a(\mathbf{r}, \mathbf{s}_m)$ , searching for  $\text{Max}[P(\mathbf{s}_m|\mathbf{r})]$  (i.e. applying the rule of MAP criterion) must be equivalent to

$$\text{Max}[P(\mathbf{s}_m|\mathbf{r})] \equiv \text{Min}[D(\mathbf{r}, \mathbf{s}_m)] \equiv \text{Min}[D^a(\mathbf{r}, \mathbf{s}_m)] \equiv \text{Max}[C(\mathbf{r}, \mathbf{s}_m)] \quad (6.9)$$

(6.9) means that our optimum detection rule is simply finding the distances between the received vector  $\mathbf{r}$  and all possible signals transmitted,  $\mathbf{s}_1 \cdots \mathbf{s}_M$  and deciding on  $\mathbf{s}_m$  which gives the minimum distance, i.e.  $\text{Min}[D^a(\mathbf{r}, \mathbf{s}_m)]$  or finding the correlation between the received vector  $\mathbf{r}$  and all possible signals transmitted,  $\mathbf{s}_1 \cdots \mathbf{s}_M$  and deciding on the one which gives the maximum correlation, i.e.  $\text{Max}[C(\mathbf{r}, \mathbf{s}_m)]$ .

The above development is valid for the situation when all signals are sent from transmitter with equal probability. If this is not the case, then we go back to (6.2) and (6.3) and keep in mind that the pdf function  $f(\mathbf{r})$  is a sum that remains constant whichever  $m$  is chosen, thus has no effect on maximization process. Under these circumstances,  $\text{Max}[P(\mathbf{s}_m|\mathbf{r})]$  will become

$$\text{Max}[P(\mathbf{s}_m|\mathbf{r})] \equiv \text{Max}[f(\mathbf{r}|\mathbf{s}_m)P(\mathbf{s}_m)] \quad (6.10)$$

It is clear that by the application of  $D^a(\mathbf{r}, \mathbf{s}_m)$  or  $C(\mathbf{r}, \mathbf{s}_m)$  we start to define an area of (correct) decision region for the signal  $s_m(t)$  which we denote by  $R_m$ . Then, the probability of error  $P_e(\mathbf{s}_m)$  for the signal  $\mathbf{s}_m$  will be given by the integration of  $f(\mathbf{r}|\mathbf{s}_m)$  over the entire area excluding the one belonging to  $R_m$ . This area is denoted by  $R_m^c$ . Then

$$P_e(\mathbf{s}_m) = \int_{R_m^c} f(\mathbf{r}|\mathbf{s}_m) d\mathbf{r} \quad (6.11)$$

The average probability of error over the total of  $M$  signals will be

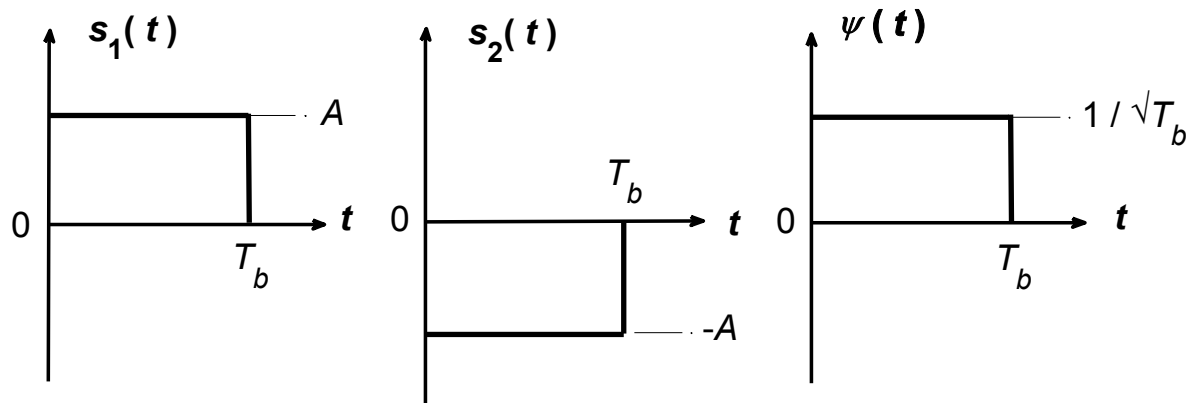
$$\begin{aligned} P_e &= \frac{1}{M} \sum_{m=1}^M P_e(\mathbf{s}_m) = \frac{1}{M} \sum_{m=1}^M \int_{R_m^c} f(\mathbf{r}|\mathbf{s}_m) d\mathbf{r} \\ &= \frac{1}{M} \sum_{m=1}^M \left[ 1 - \int_{R_m} f(\mathbf{r}|\mathbf{s}_m) d\mathbf{r} \right] \end{aligned} \quad (6.12)$$

In case the signals  $\mathbf{s}_1 \cdots \mathbf{s}_M$  are not sent with equal probability, i.e. if MAP criterion is valid, (6.12) turns into

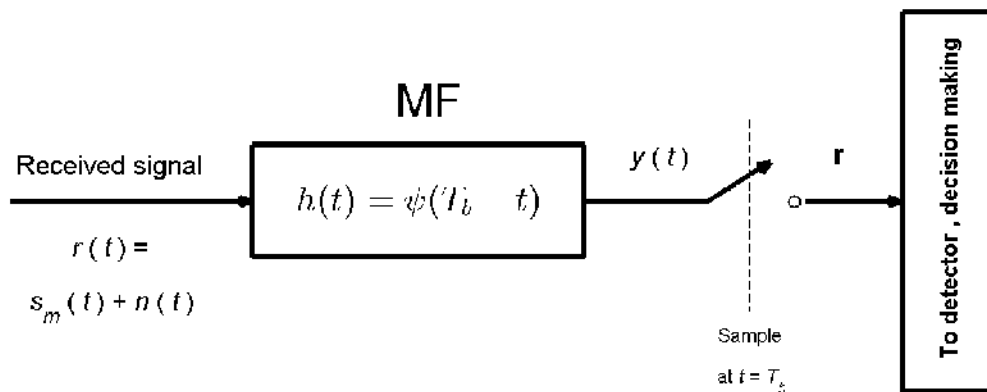
$$P_e = 1 - \sum_{m=1}^M P(\mathbf{s}_m) \int_{R_m} f(\mathbf{r} | \mathbf{s}_m) d\mathbf{r} \quad (6.13)$$

Now we solve two lengthy examples to illustrate the above points.

Example 6.1 : Consider an ASK system where  $M = 2$  and the transmitter uses the signal set and the basis function,  $s_1(t)$ ,  $s_2(t)$  and  $\psi(t)$  shown in Fig. 6.3a.  $s_1(t)$  and  $s_2(t)$  are transmitted with unequal probabilities of  $p$  and  $1-p$  respectively. Determine the metrics, i.e.,  $\text{Max}[P(\mathbf{s}_m | \mathbf{r})] \equiv \text{Max}[f(\mathbf{r} | \mathbf{s}_m)P(\mathbf{s}_m)]$  for the MAP optimum detector.



a) Transmitted signal waveforms, the basis function



b) Block diagram of MF demodulator

Fig. 6.3 Transmitted signal waveforms, the basis function and the block diagram of MF demodulator for Example 6.1.

Solution : In Fig. 6.2b, the demodulator at the receiver side is shown as matched filter (MF). Accordingly, for the cases of  $s_1(t)$  and  $s_2(t)$ ,  $y(t)$  after MF becomes the following

$$\begin{aligned}
 y_{s_1}(t) &= \int_0^t r(\tau) \psi(T_b - t + \tau) d\tau \\
 &= \int_0^t s_1(\tau) \psi(T_b - t + \tau) d\tau + \int_0^t n(\tau) \psi(T_b - t + \tau) d\tau \\
 y_{s_2}(t) &= \int_0^t r(\tau) \psi(T_b - t + \tau) d\tau \\
 &= \int_0^t s_2(\tau) \psi(T_b - t + \tau) d\tau + \int_0^t n(\tau) \psi(T_b - t + \tau) d\tau
 \end{aligned} \tag{6.14}$$

After sampling at  $t = T_b$ , (6.14) will be

$$\begin{aligned}
 y_{s_1}(T_b) &= \int_0^{T_b} s_1(\tau) \psi(\tau) d\tau + \int_0^{T_b} n(\tau) \psi(\tau) d\tau = A\sqrt{T_b} + n(T_b) = \sqrt{\varepsilon_b} + n(T_b) \\
 y_{s_2}(T_b) &= \int_0^{T_b} s_2(\tau) \psi(\tau) d\tau + \int_0^{T_b} n(\tau) \psi(\tau) d\tau = -A\sqrt{T_b} + n(T_b) = -\sqrt{\varepsilon_b} + n(T_b) \\
 n(T_b) &= \int_0^{T_b} n(\tau) \psi(\tau) d\tau \quad , \quad \varepsilon_b = \int_0^{T_b} s_1^2(t) dt = \int_0^{T_b} s_2^2(t) dt = A^2 T_b
 \end{aligned} \tag{6.15}$$

$n(T_b)$  is the noise sample that has the same characteristics of  $n(t)$  in the received signal. Thus  $n(T_b)$  is Gaussian with zero mean and variance  $\sigma_n^2 = N_0/2$ . From (5.8) and (6.15), we work out the individual  $f(r | s_1)$  and  $f(r | s_2)$  as

$$\begin{aligned}
 f(r | s_1) &= \frac{1}{(\pi N_0)^{0.5}} \exp\left[-(r - \sqrt{\varepsilon_b})^2 / N_0\right] \\
 f(r | s_2) &= \frac{1}{(\pi N_0)^{0.5}} \exp\left[-(r + \sqrt{\varepsilon_b})^2 / N_0\right]
 \end{aligned} \tag{6.16}$$

For a detection strategy based on finding  $\text{Max}[P(\mathbf{s}_m | \mathbf{r})] \equiv \text{Max}[f(\mathbf{r} | \mathbf{s}_m)P(\mathbf{s}_m)]$ , we simply decide as follows

$$\begin{aligned}
 \text{If } f(r | s_1)P(s_1) &> f(r | s_2)P(s_2) && \text{then decide } s_1(t) \text{ was transmitted} \\
 \text{If } f(r | s_1)P(s_1) &< f(r | s_2)P(s_2) && \text{then decide } s_2(t) \text{ was transmitted}
 \end{aligned} \tag{6.17}$$

Substituting from (6.16) into (6.17)

$$\begin{aligned} \text{If } r &> \frac{N_0}{4\sqrt{\varepsilon_b}} \ln\left(\frac{1-p}{p}\right) \text{ then decide } s_1(t) \text{ was transmitted} \\ \text{If } r &< \frac{N_0}{4\sqrt{\varepsilon_b}} \ln\left(\frac{1-p}{p}\right) \text{ then decide } s_2(t) \text{ was transmitted} \end{aligned} \quad (6.18)$$

So our decision requires a knowledge of  $N_0$ ,  $\varepsilon_b$  and  $p$ . It is quite possible that the transmitter sends information about the last two parameters, but  $N_0$  has to be measured somehow. Note that if  $p=0.5$ , meaning that  $s_1(t)$  and  $s_2(t)$  are sent with equal probabilities from the transmitter then the decision rule of (6.18) will become independent of the parameters as shown below.

$$\begin{aligned} \text{If } r &> 0 \text{ then decide } s_1(t) \text{ was transmitted} \\ \text{If } r &< 0 \text{ then decide } s_2(t) \text{ was transmitted} \end{aligned} \quad (6.19)$$

Example 6.2 : Give at least two different sets of time waveforms,  $s_1(t) \cdots s_4(t)$  for 4 PSK. For these waveforms, find appropriate orthonormalized basis functions, find the representation of  $s_1(t) \cdots s_4(t)$  in terms of orthonormalized basis functions, find  $\mathbf{s}_1 \cdots \mathbf{s}_4$  vectors, the distances between vector ends, draw constellation diagram and the diagram of demodulator comprising correlator and matched filter. Show that distance and correlation metrics function properly (i.e. give the correct decision) if  $s_1(t)$  was sent from the transmitter and no noise is mixed with the signal at receiver. Give correct decision boundaries and find probability of error if all signals are sent from transmitter with equal probability.

Solution : Two possible sets of  $s_1(t) \cdots s_4(t)$  and  $\psi_1(t)$ ,  $\psi_2(t)$  are given in Figs. 6.4 and 6.5

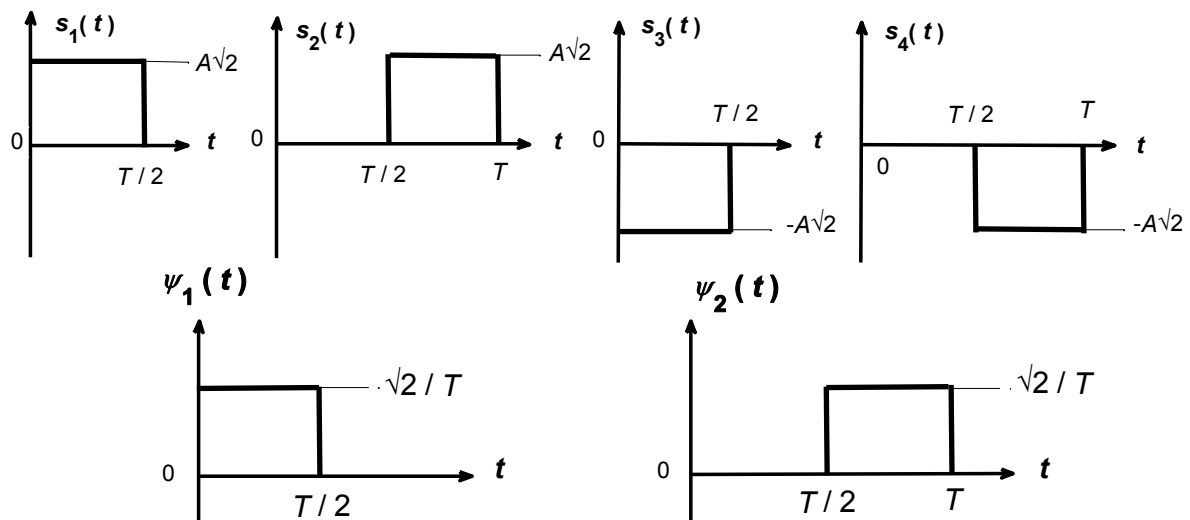


Fig. 6.4 First possible set of signal waveforms,  $s_1(t) \cdots s_4(t)$  and orthonormalized basis functions,  $\psi_1(t)$ ,  $\psi_2(t)$  for 4 PSK.

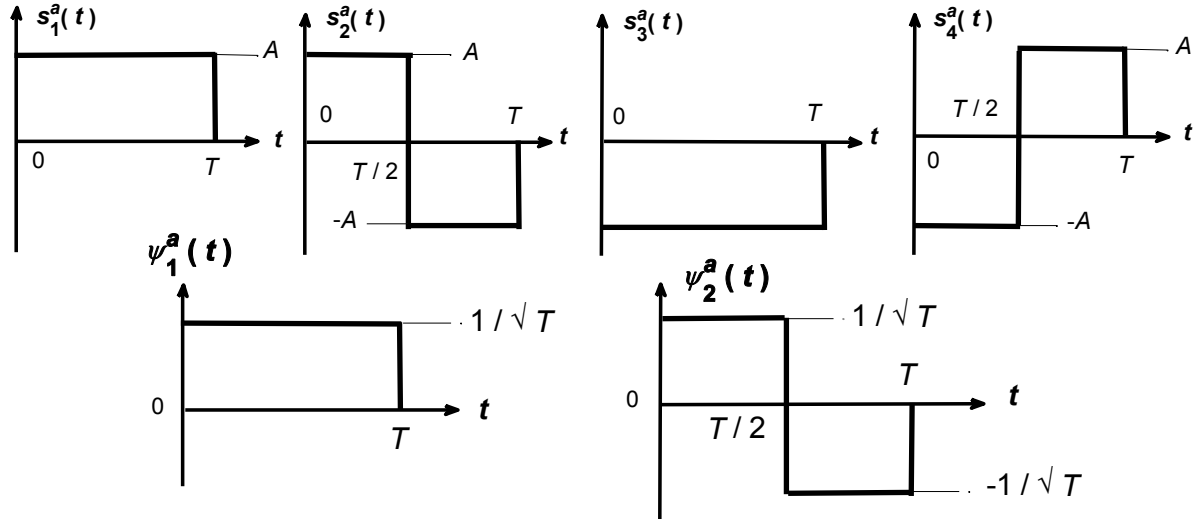


Fig. 6.5 First possible set of signal waveforms,  $s_1^a(t) \cdots s_4^a(t)$  and orthonormalized basis functions,  $\psi_1^a(t)$ ,  $\psi_2^a(t)$  for 4 PSK.

Note that signal waveforms and orthonormalized basis functions in Figs. 6.4 and 6.5 are interchangeable. Here we continue our solution with the set shown Fig. 6.4. Initially we write the time waveform expressions for  $s_1(t) \cdots s_4(t)$  and  $\psi_1(t)$ ,  $\psi_2(t)$

$$\begin{aligned}
 s_1(t) &= \begin{cases} A\sqrt{2} & 0 \leq t \leq T/2 \\ 0 & \text{otherwise} \end{cases} & s_2(t) &= \begin{cases} A\sqrt{2} & T/2 \leq t \leq T \\ 0 & \text{otherwise} \end{cases} \\
 s_3(t) &= \begin{cases} -A\sqrt{2} & 0 \leq t \leq T/2 \\ 0 & \text{otherwise} \end{cases} & s_4(t) &= \begin{cases} -A\sqrt{2} & T/2 \leq t \leq T \\ 0 & \text{otherwise} \end{cases} \\
 \psi_1(t) &= \begin{cases} \sqrt{2/T} & 0 \leq t \leq T/2 \\ 0 & \text{otherwise} \end{cases} & \psi_2(t) &= \begin{cases} \sqrt{2/T} & T/2 \leq t \leq T \\ 0 & \text{otherwise} \end{cases} \quad (6.20)
 \end{aligned}$$

Now either by eye inspection or by **Gram-Schmidt Orthogonalization Procedure**, we write  $s_1(t) \cdots s_4(t)$  in terms of  $\psi_1(t)$  and  $\psi_2(t)$ . Note that here there is no need to indicate the time intervals, since they are embedded in  $\psi_1(t)$  and  $\psi_2(t)$

$$\begin{aligned}
 s_1(t) &= A\sqrt{T}\psi_1(t) \quad , \quad s_2(t) = A\sqrt{T}\psi_2(t) \quad , \quad s_3(t) = -A\sqrt{T}\psi_1(t) \quad , \quad s_4(t) = -A\sqrt{T}\psi_2(t) \\
 \mathbf{s}_1 &= [s_{11}, s_{12}] = [A\sqrt{T}, 0] \quad , \quad \mathbf{s}_2 = [s_{21}, s_{22}] = [0, A\sqrt{T}] \\
 \mathbf{s}_3 &= [s_{31}, s_{32}] = [-A\sqrt{T}, 0] \quad , \quad \mathbf{s}_4 = [s_{41}, s_{42}] = [0, -A\sqrt{T}] \\
 d_{12} &= d_{14} = d_{23} = A\sqrt{2T} = \sqrt{2\varepsilon_s} \quad , \quad d_{13} = d_{24} = 2A\sqrt{T} = 2\sqrt{\varepsilon_s} \\
 |\mathbf{s}_1| &= |\mathbf{s}_2| = |\mathbf{s}_3| = |\mathbf{s}_4| = A\sqrt{T} \quad , \quad \varepsilon_1 = \varepsilon_2 = \varepsilon_3 = \varepsilon_4 = \varepsilon_s = A^2T \quad (6.21)
 \end{aligned}$$

On the second and third lines of (6.21), we have included the vectorial representation of our signals, on the fourth line we have given the respective distance between vector ends, on the last line the

length of vectors and the energies are given which can be calculated either from time signals or vectorial representations. As this is PSK, all vector lengths, thus the energies are equal. Now we can plot the constellation diagram of  $s_1 \dots s_4$ . This is illustrated in Fig. 6.6

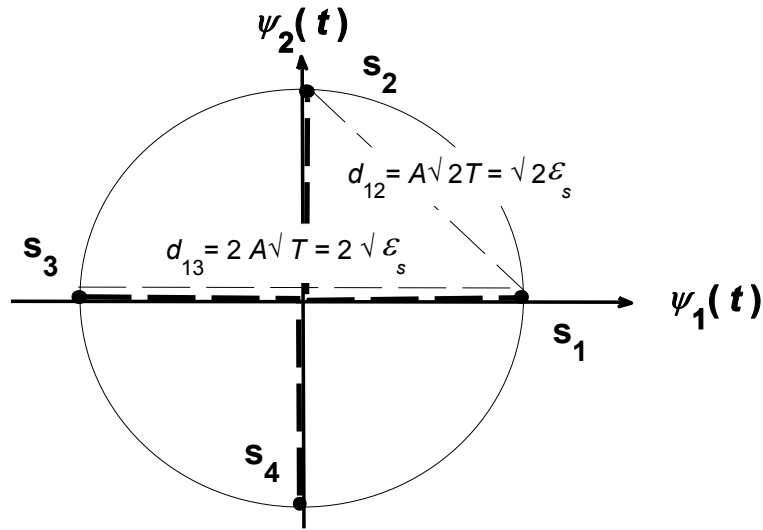
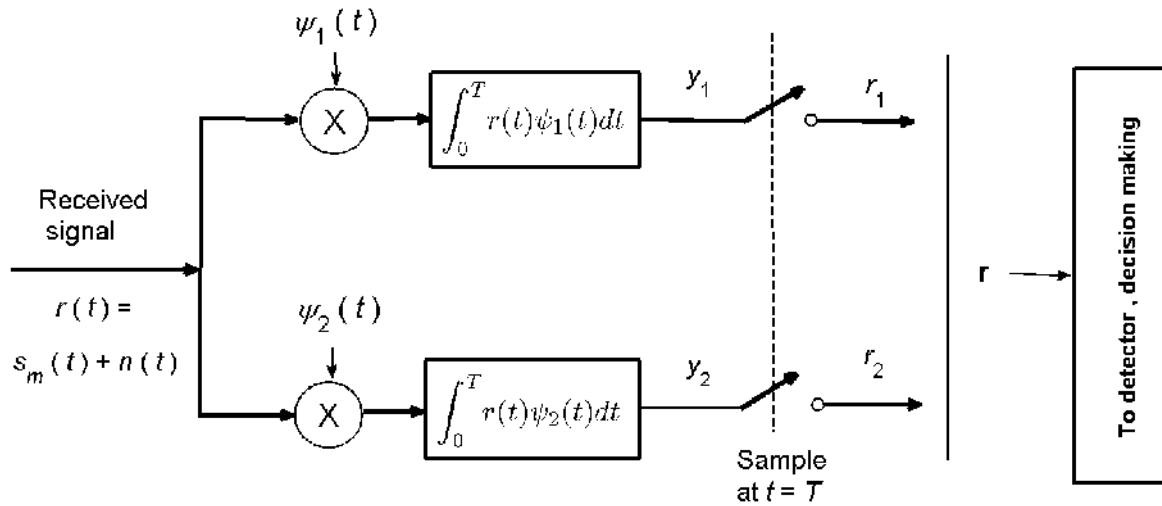
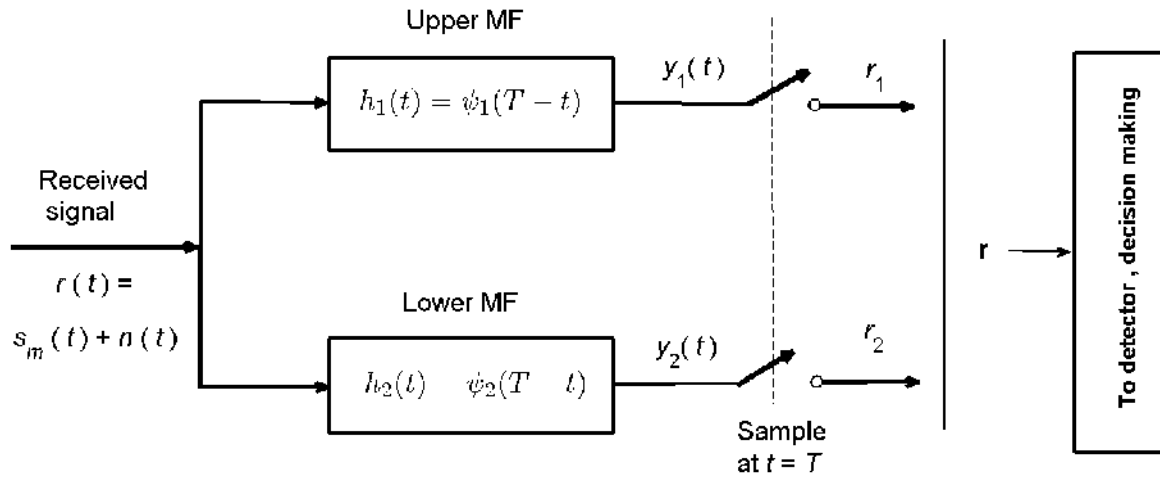


Fig. 6.6 Constellation diagram for the 4 PSK in Example 6.2.

Below, we show the block diagrams of correlator and matched filter type of demodulators.



a) Block diagram of correlator type of demodulator.



b) Block diagram of matched filter type of demodulator.

Fig. 6. 7 Block diagrams of correlator and matched filter type of demodulators for the 4 PSK in Example 6.2.

We first tackle the case of the correlator and assume that  $s_1(t)$  was sent from the transmitter

$$\begin{aligned}
 y_1 = r_1 &= \int_0^T r(t) \psi_1(t) dt = \int_0^T s_1(t) \psi_1(t) dt + \int_0^T n(t) \psi_1(t) dt \\
 &= A\sqrt{T} + n_1, \quad n_1 = \int_0^T n(t) \psi_1(t) dt \\
 y_2 = r_2 &= \int_0^T r(t) \psi_2(t) dt = \int_0^T s_1(t) \psi_2(t) dt + \int_0^T n(t) \psi_2(t) dt \\
 &= 0 + n_2, \quad n_2 = \int_0^T n(t) \psi_2(t) dt, \quad \mathbf{r} = [r_1; r_2]
 \end{aligned} \tag{6.22}$$

The reason that we have arranged vector  $\mathbf{r}$  in the form of a column vector rather than a row vector, is because column arrangement facilitates metrics computation.

Doing the same for the matched filter case, we get

$$\begin{aligned}
 y_1(t) &= \int_0^t r(\tau) h_1(t-\tau) d\tau = \int_0^t r(\tau) \psi_1(T-t+\tau) d\tau \\
 &= \int_0^t s_1(\tau) \psi_1(T-t+\tau) d\tau + \int_0^t n(\tau) \psi_1(T-t+\tau) d\tau \\
 y_2(t) &= \int_0^t r(\tau) h_2(t-\tau) d\tau = \int_0^t r(\tau) \psi_2(T-t+\tau) d\tau \\
 &= \int_0^t s_1(\tau) \psi_2(T-t+\tau) d\tau + \int_0^t n(\tau) \psi_2(T-t+\tau) d\tau
 \end{aligned} \tag{6.23}$$

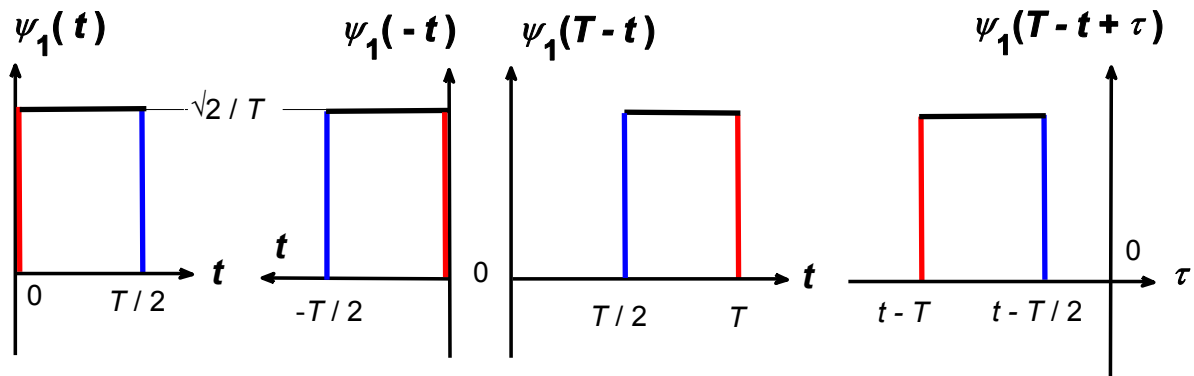
After sampling at  $t = T$ , (6.23) will become



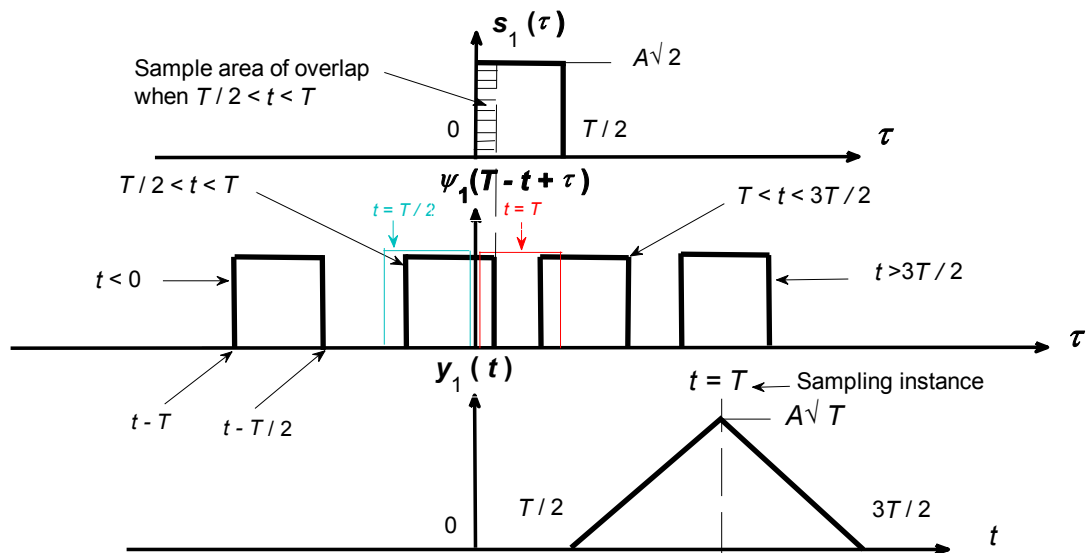
$$r_1 = y_1(T) = \int_0^T r(\tau) \psi_1(\tau) d\tau = \overbrace{A\sqrt{T}}^{\text{signal part}} + \overbrace{\hat{n}_1}^{\text{noise part}} = \sqrt{\varepsilon_s} + n_1, \quad n_1 = \int_0^T n(t) \psi_1(t) dt$$

$$r_2 = y_2(T) = \int_0^T r(\tau) \psi_2(\tau) d\tau = \overbrace{0}^{\text{signal part}} + \overbrace{\hat{n}_2}^{\text{noise part}}, \quad n_2 = \int_0^T n(t) \psi_2(t) dt, \quad \mathbf{r} = [r_1; r_2] \quad (6.24)$$

So the outputs, we obtain from correlator and matched filter are the same. For the case of matched filter demodulator, it is instructive to graphically illustrate the convolution operation carried out in  $y_1(t)$  and  $y_2(t)$  of (6.23) for the signal parts. For the upper and lower branches of Fig. 6.7 a, this is respectively done in Figs. 6.8 and 6.9.

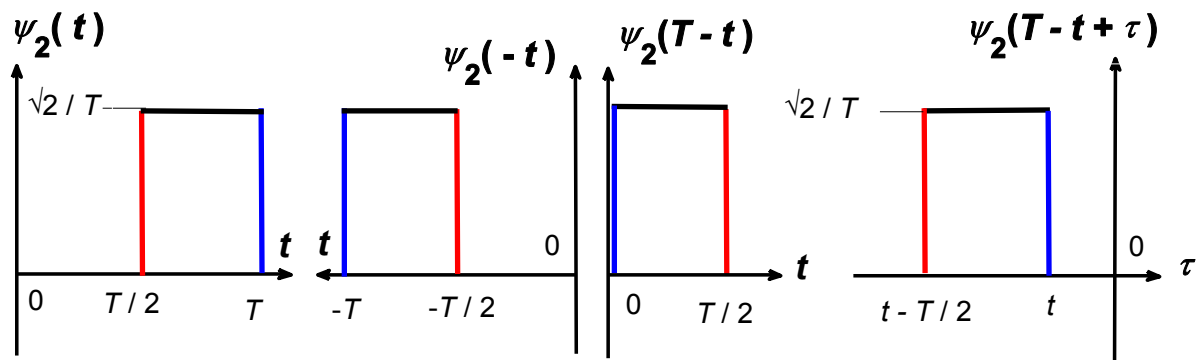


a) Orientation of matched filter (MF)  $\psi_1(t)$  for convolution operation in Fig. 6.7b



b) Output from matched filter (MF)  $\psi_1(t)$  via convolution

Fig. 6. 8 Graphical illustration of the convolution operation implemented in the upper matched filter of Fig. 6.7b.



a) Orientation of matched filter (MF)  $\psi_2(t)$  for convolution operation in

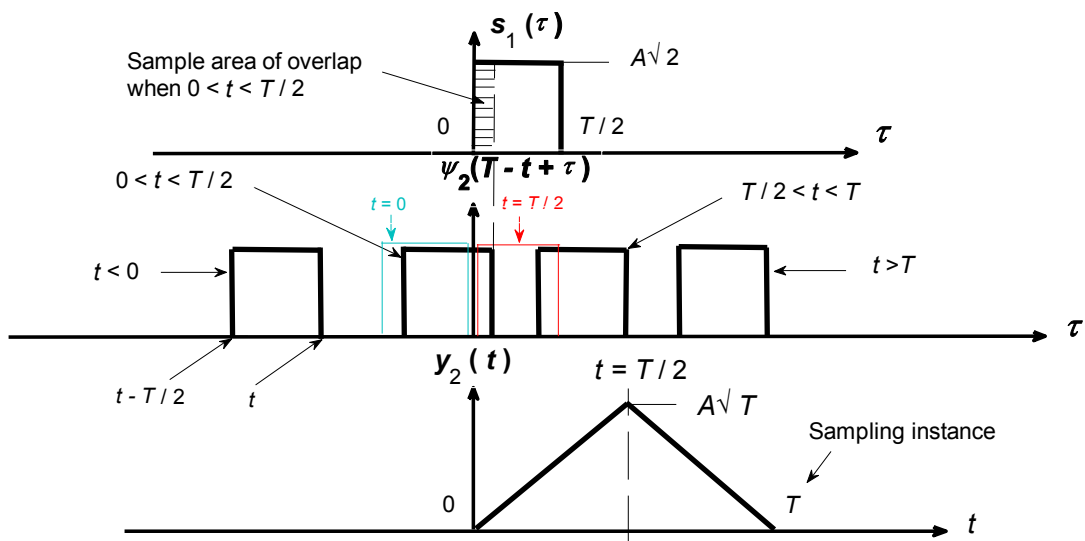


Fig. 6.7b

b) Output from matched filter (MF)  $\psi_1(t)$  via convolution

Fig. 6. 9 Graphical illustration of the convolution operation implemented in the lower matched filter of Fig. 6.7b.

Now we compute correlation metrics values by inserting  $s_1 \dots s_4$  into  $C(\mathbf{r}, \mathbf{s}_m)$ . From (6.8) and (6.22), we have

$$\begin{aligned}
m=1, C(\mathbf{r}, \mathbf{s}_1) &= 2\mathbf{s}_1 \cdot \mathbf{r} - \|\mathbf{s}_1\|^2 = 2[A\sqrt{T}, 0] \begin{bmatrix} A\sqrt{T} + n_1 \\ n_2 \end{bmatrix} - A^2T = A^2T + 2An_1\sqrt{T} \\
m=2, C(\mathbf{r}, \mathbf{s}_2) &= 2\mathbf{s}_2 \cdot \mathbf{r} - \|\mathbf{s}_2\|^2 = 2[0, A\sqrt{T}] \begin{bmatrix} A\sqrt{T} + n_1 \\ n_2 \end{bmatrix} - A^2T = 2An_2\sqrt{T} - A^2T \\
m=3, C(\mathbf{r}, \mathbf{s}_3) &= 2\mathbf{s}_3 \cdot \mathbf{r} - \|\mathbf{s}_3\|^2 = 2[-A\sqrt{T}, 0] \begin{bmatrix} A\sqrt{T} + n_1 \\ n_2 \end{bmatrix} - A^2T = -3A^2T - 2An_1\sqrt{T} \\
m=4, C(\mathbf{r}, \mathbf{s}_4) &= 2\mathbf{s}_4 \cdot \mathbf{r} - \|\mathbf{s}_4\|^2 = 2[0, -A\sqrt{T}] \begin{bmatrix} A\sqrt{T} + n_1 \\ n_2 \end{bmatrix} - A^2T = -2An_2\sqrt{T} - A^2T \quad (6.25)
\end{aligned}$$

It is clear from (6.25) that in the absence of noise i.e.  $n_1 = n_2 = 0$ ,  $C(\mathbf{r}, \mathbf{s}_1)$  becomes the largest in the set of  $C(\mathbf{r}, \mathbf{s}_m)$ ,  $m=1 \dots 4$ . Under such circumstances, the detector correctly decides that  $s_1(t)$  was transmitted. In the presence of noise, to arrive at a correct decision, it must be that

$$\begin{aligned}
&C(\mathbf{r}, \mathbf{s}_1) > C(\mathbf{r}, \mathbf{s}_2), C(\mathbf{r}, \mathbf{s}_1) > C(\mathbf{r}, \mathbf{s}_3), C(\mathbf{r}, \mathbf{s}_1) > C(\mathbf{r}, \mathbf{s}_4) \\
\text{or } \text{Max}[C(\mathbf{r}, \mathbf{s}_1), C(\mathbf{r}, \mathbf{s}_2), C(\mathbf{r}, \mathbf{s}_3), C(\mathbf{r}, \mathbf{s}_4)] &= C(\mathbf{r}, \mathbf{s}_1) \quad (6.26)
\end{aligned}$$

These three conditions correspond to

$$\begin{aligned}
C(\mathbf{r}, \mathbf{s}_1) > C(\mathbf{r}, \mathbf{s}_2) &: A^2T + 2An_1\sqrt{T} > 2An_2\sqrt{T} - A^2T \rightarrow A\sqrt{T} + n_1 > n_2 \\
C(\mathbf{r}, \mathbf{s}_1) > C(\mathbf{r}, \mathbf{s}_3) &: A^2T + 2An_1\sqrt{T} > -3A^2T - 2An_1\sqrt{T} \rightarrow A\sqrt{T} > -n_1 \\
C(\mathbf{r}, \mathbf{s}_1) > C(\mathbf{r}, \mathbf{s}_4) &: A^2T + 2An_1\sqrt{T} > -2An_2\sqrt{T} - A^2T \rightarrow A\sqrt{T} + n_1 > -n_2 \quad (6.27)
\end{aligned}$$

From (6.24) and Fig. 6.6, we deduce that if  $s_1(t)$  was transmitted and gets mixed with noise, then the input to the decision making device (detector) will look like the following

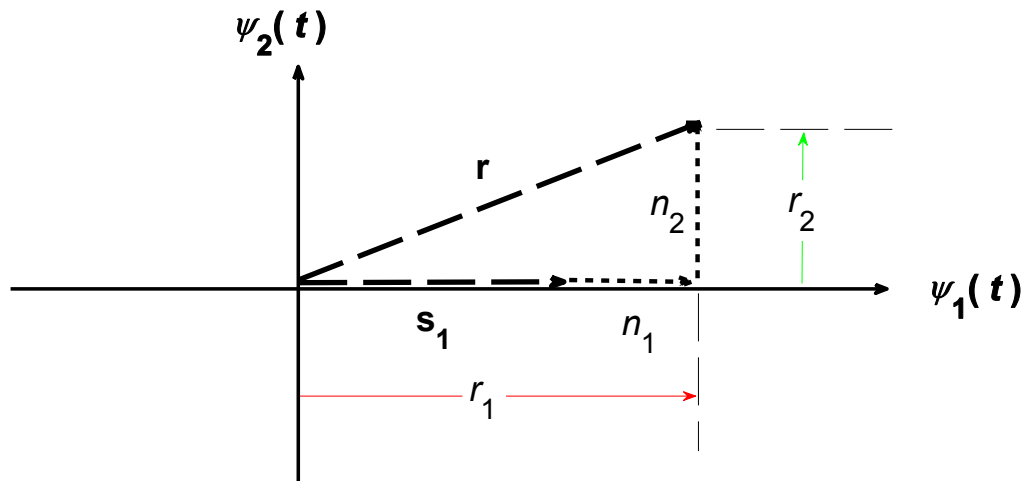


Fig. 6. 10 The input to the decision making device if  $s_1(t)$  was transmitted.

The three conditions in (6.27) individually define the regions shown in Fig. 6.11.

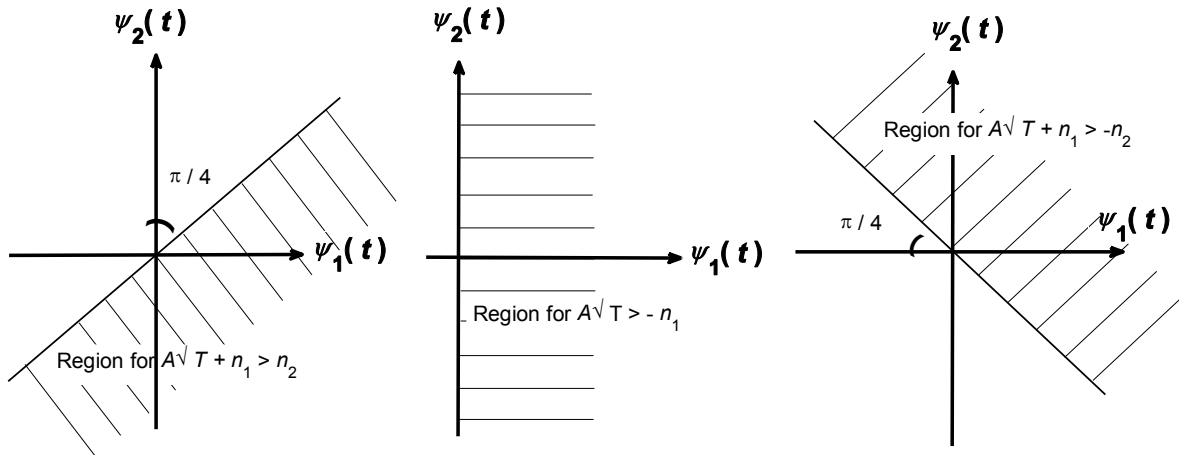


Fig. 6. 11 Regions for conditions in (6.27).

Since conditions in (6.27) are connected by AND relation, then the intersection of the three regions of Fig. 6.11 becomes

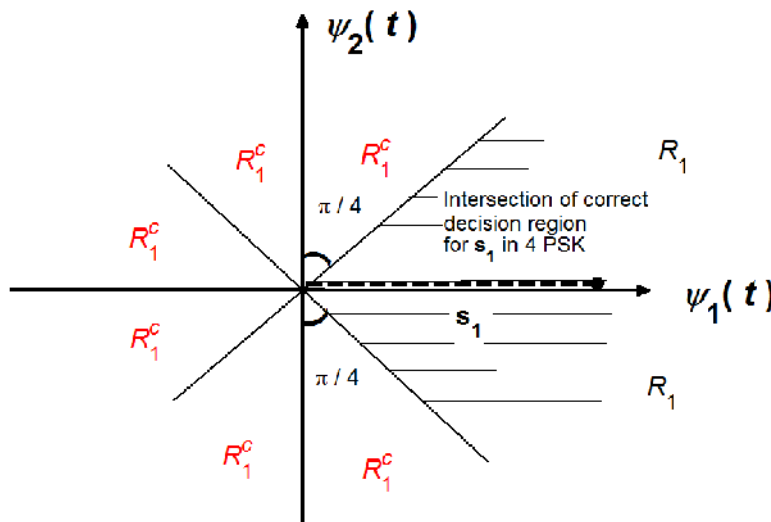


Fig. 6. 12 Intersection of correct decision region for conditions in (6.27).

With the view in Fig. 6.12, we are now in a position to estimate the probability of error for 4 PSK or  $M$  ary PSK in general. For simplicity, here we choose to find the probability of correct detection  $P_c$  and use it to find the probability of error  $P_e$  from the following relation

$$P_e = 1 - P_c \quad (6.28)$$

The conditions in (6.27) may be written in a different way, taking into account Fig. 6. 12, that is

$$-\frac{\pi}{4} < \tan^{-1}\left(\frac{n_2}{n_1 + \sqrt{\varepsilon_s}}\right) < \frac{\pi}{4}, \quad n_1 > -\sqrt{\varepsilon_s}, \quad \varepsilon_s = A^2T \quad (6.29)$$

where we have used the alternative definition of  $\varepsilon_s = A^2T$ . The first inequality in (6.29) is a combination of first and third conditions from (6.27), while the second inequality of (6.29) is merely the second condition from (6.27) expressed in a different manner. Writing (6.29) purely in terms of  $n_1$  and  $n_2$ , we get

$$-(n_1 + \sqrt{\varepsilon_s}) \tan\left(\frac{\pi}{4}\right) < n_2 < (n_1 + \sqrt{\varepsilon_s}) \tan\left(\frac{\pi}{4}\right), \quad n_1 > -\sqrt{\varepsilon_s} \quad (6.30)$$

So we can utilize the noise pdf definition given in (5.6) and set  $P_c$  as follows

$$P_c = \frac{1}{(\pi N_0)^{0.5}} \int_{-\sqrt{\varepsilon_s}}^{\infty} \exp\left(-\frac{n_1^2}{N_0}\right) dn_1 \frac{1}{(\pi N_0)^{0.5}} \int_{-(n_1 + \sqrt{\varepsilon_s}) \tan\left(\frac{\pi}{4}\right)}^{(n_1 + \sqrt{\varepsilon_s}) \tan\left(\frac{\pi}{4}\right)} \exp\left(-\frac{n_2^2}{N_0}\right) dn_2 \quad (6.31)$$

Note that in the general case of  $M$  ary PSK, (6.31) simply becomes

$$P_c = \frac{1}{(\pi N_0)^{0.5}} \int_{-\sqrt{\varepsilon_s}}^{\infty} \exp\left(-\frac{n_1^2}{N_0}\right) dn_1 \frac{1}{(\pi N_0)^{0.5}} \int_{-(n_1 + \sqrt{\varepsilon_s}) \tan\left(\frac{\pi}{M}\right)}^{(n_1 + \sqrt{\varepsilon_s}) \tan\left(\frac{\pi}{M}\right)} \exp\left(-\frac{n_2^2}{N_0}\right) dn_2 \quad (6.32)$$

The evaluation of  $P_e$  for the cases of  $M = 2$  and general  $M$  are given below

$$\begin{aligned} M = 2, P_e &= Q\left(\sqrt{\frac{2\varepsilon_s}{N_0}}\right), \quad \text{SNR}_s = \frac{\varepsilon_s}{N_0}, \quad \text{SNR}_b = \frac{\varepsilon_s}{\log_2(M)N_0} = \frac{\varepsilon_b}{N_0} \\ \text{Any } M, P_e &= 1 - \frac{1}{\pi^{0.5}} \exp(-\text{SNR}_s) \int_0^{\infty} \exp(-z^2 + 2z\text{SNR}_s^{0.5}) \text{erf}\left[z \tan\left(\frac{\pi}{M}\right)\right] dz \\ Q(x) &= \frac{1}{(2\pi)^{0.5}} \int_x^{\infty} \exp\left(-\frac{z^2}{2}\right) dz, \quad \Phi(x) = \frac{1}{(2\pi)^{0.5}} \int_{-\infty}^x \exp\left(-\frac{z^2}{2}\right) dz \\ Q(x) + \Phi(x) &= 1, \quad \Phi(x) = Q(-x), \quad \text{erf}(x) + \text{erfc}(x) = 1 \\ \text{erf}(x) &= \frac{2}{\pi^{0.5}} \int_0^x \exp(-z^2) dz, \quad \text{erfc}(x) = \frac{2}{\pi^{0.5}} \int_x^{\infty} \exp(-z^2) dz \\ Q(x) &= 0.5\text{erfc}(x/2^{0.5}) = 0.5 - 0.5\text{erf}(x/2^{0.5}), \quad Q(x) \approx \frac{1}{x\sqrt{2\pi}} \exp(-x^2/2), \quad x > 3 \\ \Phi(x) &= 1 - \text{erfc}(x/2^{0.5}) = 0.5 - 0.5\text{erf}(x/2^{0.5}) \end{aligned} \quad (6.33)$$

As seen from (6.33), it is possible to evaluate  $P_e$  analytically only in the case of  $M = 2$ , for  $M > 2$ , numeric evaluation is required.  $\Phi(x)$  and  $Q(x)$  are known as error function and complimentary error function respectively. Their definitions are slightly different in Matlab denoted as

$\text{erf}(x)$  and  $\text{erfc}(x)$ . The equivalences are given on the last but two lines of (6.33). SNR is the signal to noise ratio. As given in (6.33), it is signal energy divided by noise spectral density, sometimes it is taken as signal power divided by noise power. When signal part refers to symbol energy, we put the subscript  $s$ , but if it's the energy in the binary waveform, then we use the subscript  $b$ .

Finally we want to point out that the  $P_c$  and  $P_e$  derivations made above for the case of  $\mathbf{s}_1$  actually represents the general case of any  $\mathbf{s}_m$  and the total average  $P_c$  and  $P_e$ , since

$$\begin{aligned}
 P_c(\text{Average}) &= P(\mathbf{s}_1 \text{ being sent})P(\mathbf{r} \text{ falling in correct decision of } \mathbf{s}_1) \\
 &\quad + P(\mathbf{s}_2 \text{ being sent})P(\mathbf{r} \text{ falling in correct decision of } \mathbf{s}_2) \\
 &\quad \cdot \qquad \qquad \qquad \cdot \qquad \qquad \qquad \cdot \\
 &\quad \cdot \qquad \qquad \qquad \cdot \qquad \qquad \qquad \cdot \\
 &\quad \cdot \qquad \qquad \qquad \cdot \qquad \qquad \qquad \cdot \\
 &\quad + P(\mathbf{s}_M \text{ being sent})P(\mathbf{r} \text{ falling in correct decision of } \mathbf{s}_M) \\
 &= P_c(\mathbf{r} \text{ falling in correct decision of } \mathbf{s}_m | \text{given } \mathbf{s}_m \text{ was sent from transmitter}) \quad (6.34)
 \end{aligned}$$

The last line in (6.34) is due to the fact that

$$P(\mathbf{s}_1 \text{ being sent}) = P(\mathbf{s}_2 \text{ being sent}) = \dots = P(\mathbf{s}_M \text{ being sent}) = \frac{1}{M} \quad (6.35)$$

Exercise 6. 1 : On the course webpage, there is the MATLAB code MallPeMdl\_2012.m to evaluate theoretical and experimental  $P_e$  for ASK, PSK, rectangular QAM using the model file modulators and demodulators called Allmodd.mdl and AllDmodd.mdl together with the associated m files of MallPeMdl\_2012.m, PeMaryPSK.m and quade.m. For the theoretical formulation, for PSK for instance, we use the second line of (6.30). To arrive at experimental  $P_e$ , we simply transmit a number of symbols of the related modulation type, then add noise to these symbols in the defined SNR ratio, then perform demodulation. In the end, the following ratio is calculated to get experimental  $P_e$

$$(\text{experimental}) P_e = \frac{\text{Number of symbols in error}}{\text{Total number of symbols transmitted } (n_s)} \quad (6.36)$$

Here care must be taken to send sufficient number of symbols so we can represent the small  $P_e$  values properly. If this is not done, fluctuations occur on probability of error curves and small  $P_e$  values will be absent from the graph. Usually the golden rule is

$$n_s \geq 10/P_e \quad (6.37)$$

By using the MATLAB code and the model files, find the  $P_e$  curves at  $M = 2, 4, 8, 32, 64, 128$  for ASK, PSK, QAM. Compare your results with Figs. 7.55, 7.57 and 7.62 of Proakis 2002. Make comments

the dependency of  $P_e$  on  $M$ ,  $n_s$  and modulation type. Explain why theoretical and experimental curves differ in some runs. Sample graphs are provided below in Fig. 6.13 and 6.14 for  $M = 4$  and  $M = 16$ .

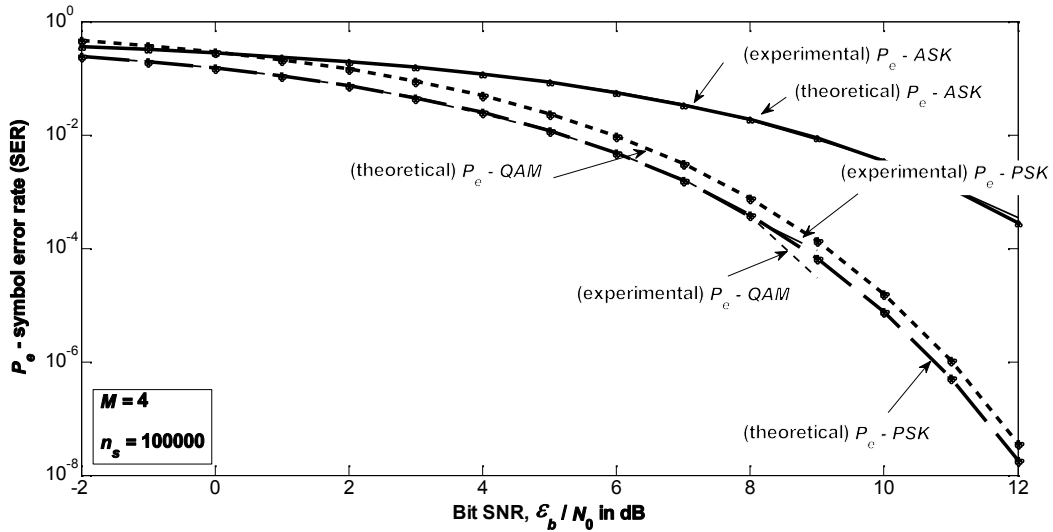


Fig. 6.13 Sample probability of error graph for ASK, PSK, QAM at  $M = 4$ .

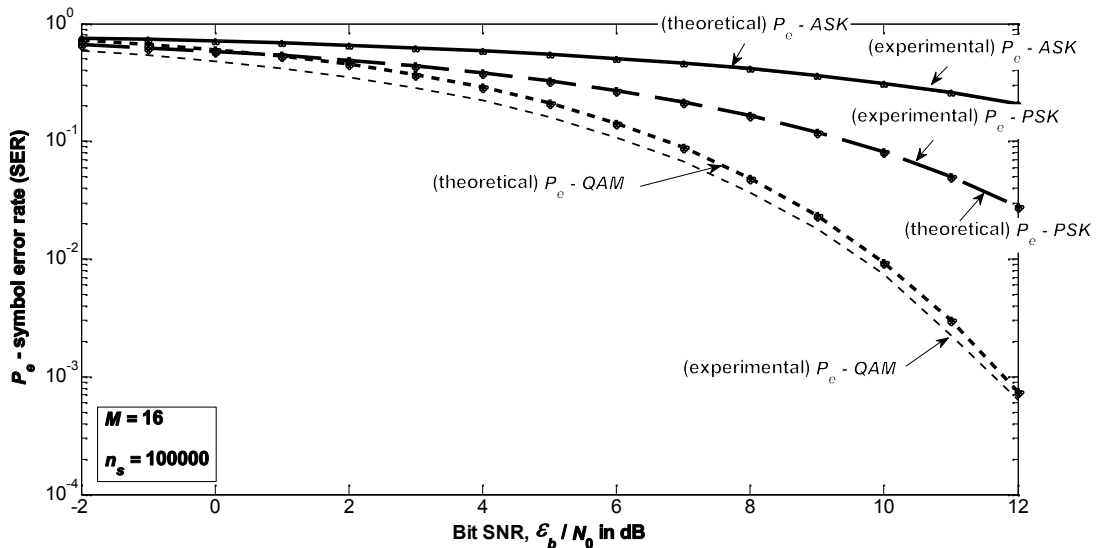


Fig. 6.14 Sample probability of error graph for ASK, PSK, QAM at  $M = 16$ .

Exercise 6.2 : By using the analysis in Example 6.2, find by hand derivation,  $P_e$  for the two PSK constellations of  $M = 2$  shown in Figs. 6.15 and 6.16. Explain the difference between the two cases.

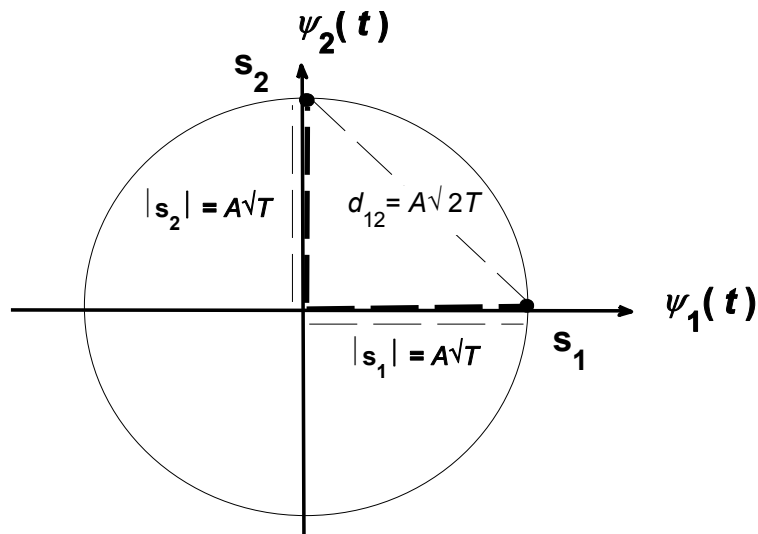


Fig. 6.15 Orthogonal PSK constellation of  $M = 2$  for Exercise 6.2.

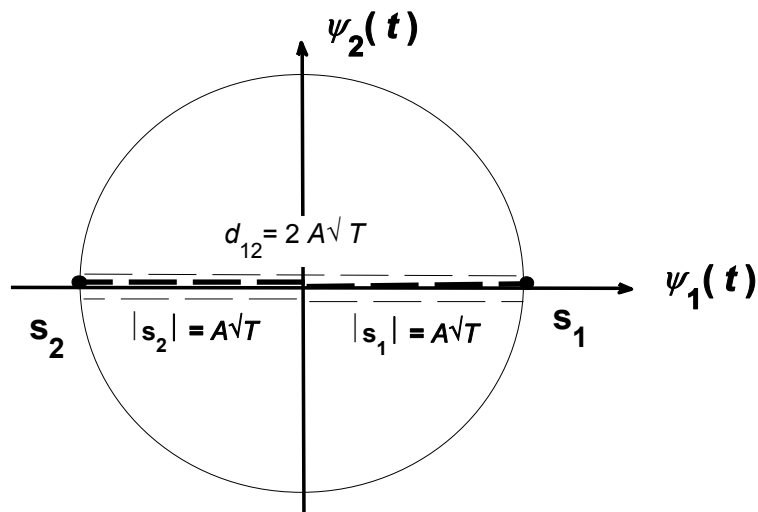


Fig. 6.16 Antipodal PSK constellation of  $M = 2$  for Exercise 6.2.

## 7. Probability of Error Calculations for ASK

Finding the probability of error for ASK requires special consideration, since as seen from Fig. 2.1 and the expressions given in (2.1), ASK signal vectors have different energies. Assuming we adjust the distance between the neighbouring signal vector ends to be equal and the energy of the smallest signal vector to be  $\varepsilon_s = A^2T$ , then for  $M$  ary ASK, we will have the following constellation



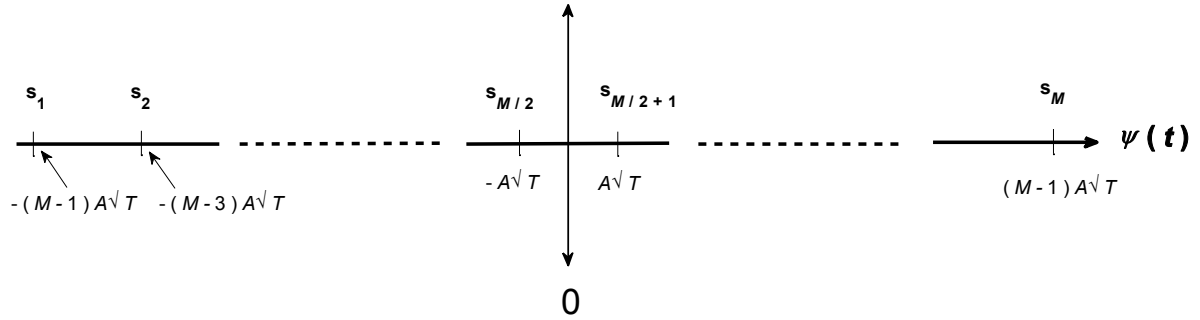


Fig. 7.1 ASK constellation for a general  $M$  ary ASK case.

From Fig. 7.1, we can write the signal vector representation as

$$\begin{aligned}
 \psi(t) &= 1/\sqrt{T} \quad 0 \leq t \leq T, \quad \varepsilon_s = \|\mathbf{s}_{M/2}\|^2 = A^2T \\
 s_1(t) &= -(M-1)A, \quad s_2(t) = -(M-3)A \quad 0 \leq t \leq T \\
 &\cdot \\
 &\cdot \\
 &\cdot \\
 s_{M-1}(t) &= (M-3)A, \quad s_M(t) = (M-1)A \quad 0 \leq t \leq T \\
 s_1(t) &= -(M-1)A\sqrt{T}\psi(t), \quad s_2(t) = -(M-3)A\sqrt{T}\psi(t) \\
 &\cdot \\
 &\cdot \\
 &\cdot \\
 s_m(t) &= (2m-1-M)A\sqrt{T}\psi(t) \\
 &\cdot \\
 &\cdot \\
 &\cdot \\
 s_{M-1}(t) &= (M-3)A\sqrt{T}\psi(t), \quad s_M(t) = (M-1)A\sqrt{T}\psi(t) \\
 \mathbf{s}_1 &= [-(M-1)A\sqrt{T}] = [-(M-1)\varepsilon_s], \quad \mathbf{s}_2 = [-(M-3)A\sqrt{T}] = [-(M-3)\varepsilon_s] \\
 &\cdot \\
 &\cdot \\
 &\cdot \\
 \mathbf{s}_{M-1} &= [(M-3)A\sqrt{T}] = [(M-3)\varepsilon_s], \quad \mathbf{s}_M = [(M-1)A\sqrt{T}] = [(M-1)\varepsilon_s] \quad (7.1)
 \end{aligned}$$

As seen from Fig. 7.1 and the arrangements in (7.1), there is a distance of  $2\varepsilon_s$  between all neighbouring signal vector ends, thus all decision regions resemble the case of the two signal vector around 0, where there is the signal vector  $\mathbf{s}_{M/2}$  to the left (negative) side and signal vector  $\mathbf{s}_{M/2+1}$  to the right (positive) side. The only exceptions are  $\mathbf{s}_1$  and  $\mathbf{s}_M$  whose one sides go to infinity. If we

imagine an artificial link between from  $\mathbf{s}_1$  to  $\mathbf{s}_M$ , then we will have  $M$  signals and  $M - 1$  identical decision regions. Based on this observation, and using the result of Exercise 6.2, we can write for the probability error for  $M$  ary ASK

$$P_{eASK} = \frac{M-1}{M} \left\{ \frac{1}{(\pi N_0)^{0.5}} \left[ \int_{\sqrt{\varepsilon_s}}^{\infty} \exp\left(-\frac{n_1^2}{N_0}\right) dn_1 + \int_{-\infty}^{-\sqrt{\varepsilon_s}} \exp\left(-\frac{n_1^2}{N_0}\right) dn_1 \right] \right\}$$

$$P_{eASK} = \frac{2(M-1)}{M} Q\left(\sqrt{\frac{2\varepsilon_s}{N_0}}\right) \quad (7.2)$$

The above text is based on

- 1) John G. Proakis, Masoud Salehi, "Communication Systems Engineering" 2<sup>nd</sup> Ed. 2002, ISBN : 0-13-061793-8.
- 2) My own lecture notes.